PROCESSING AND CHARACTERIZATION OF PVDF, PVDF-TrFE, AND PVDF-TrFE-PZT COMPOSITES

by

JARED JAMES STROYAN

A thesis submitted in partial fulfillment of
the requirements for the degree of

MASTER OF SCIENCE IN MATERIALS SCIENCE ENGINEERING

WASHINGTON STATE UNIVERSITY
School of Mechanical and Materials Engineering

DECEMBER 2004

To the Faculty of Washington State University:

The members of the Committee appointed to examine the thesis of JARED JAMES STROYAN find it satisfactory and recommend that it be accepted.

_____
Chair

_____

_____

ACKNOWLEDGMENT

I would first like to thank my advisor and committee chair, Dr. Amit Bandyopadhyay, for offering me a graduate level position and helping to guide my research at Washington State University. I greatly appreciate his willingness to work with my transferring from Eastern Washington University, and also for his understanding and patience throughout my time spent at WSU. Dr. Bandyopadhyay welcomed me to WSU as a new student, and introduced me to university level research while I was finishing undergraduate courses. I began lab work in the Ceramic Processing and Rapid Prototyping (CPRP) lab during my first semester at WSU, working on metal-ceramic composites. My studies transformed into Piezoelectric Polymers and Composites during my second semester at WSU. At this time, Dr. Susmita Bose also became equally helpful with her guidance and knowledge. I would like to thank Dr. Bose for her support and encouragement during my research. I must also thank Dr. Jow-Lian Ding. Dr. Ding guided my first Teaching Assistant position, and has been a very supportive instructor and committee member. I would like to thank J&W Medical LLC for their time and efforts involved in testing several particular samples. I also appreciate the time and advice of Henry Ruff for helping me to create various experimental setups. Many friends, group members and fellow graduate students are also acknowledged for their incites and additions to my research and education; without their support and companionship I would not have had the same experience. Lastly, I would like to give special thanks to my family. They have certainly influenced and supported me throughout my undergraduate and graduate studies.

PROCESSING AND CHARACTERIZATION OF PVDF, PVDF-TrFE,

AND PVDF-TrFE-PZT COMPOSITES

ABSTRACT

By Jared James Stroyan, M.S.
Washington State University
December 2004

Chair: Amit Bandyopadhyay

Polyvinylidene Fluoride (PVDF) is one of the few piezoelectrically active semi-crystalline polymer materials; however, the piezoelectric response of PVDF is quite minimal in relation to that of most piezoelectric ceramics. It is evident though, that copolymers such as trifluoroethylene (TrFE) and tetrafluoroethylene (TFE) help to improve the piezoelectric response in PVDF by improving the crystallinity. Further improvements can be made by producing a 0-3 composite material with a highly piezoelectric ceramic, such as lead zirconate titanate (PZT), and PVDF.

Logically, piezoelectric ceramic materials are excellent candidates for use in solid-state applications like transducers and micro-electrical-mechanical devices. However, two limiting factors of piezoelectric ceramics are the high stiffness and the relatively higher cost of fabrication. These are the primary reasons that piezoelectric polymers have been studied so extensively. Piezoelectric polymers are very flexible, easy to fabricate, and have an acoustic impedance comparable to soft human tissue. Ultimately, a material with the mechanical properties of a polymer like PVDF, and the piezoelectric

properties of a ceramic like PZT, would be ideal for many piezoelectric applications. The goals of this research project are based on these ideas, and the applications of such a material.

The primary achievements of this research are the development of the processing science necessary to create such a composite, and characterization of these composites. Bulk samples were initially developed, but characterization was not feasible due to the large electric fields required to produce piezoelectric effects in such materials. Film samples were later developed, allowing us to use the same maximum voltages available for testing, while producing a higher electric field on these thinner samples. Results of these tests confirm that the addition of PZT to PVDF/TrFE does notably improve the piezoelectric and dielectric response. A maximum peak polarization of nearly 2 $\mu C/cm^2$ has been produced from a 20 μm thick composite film with an applied electric field of 15.5 kV/cm. This is over 7.5 times the peak polarization of a similar thickness copolymer sample with about the same electric field.

TABLE OF CONTENTS

Page

LIST OF TABLES

LIST OF FIGURES

Dedication

This thesis is dedicated to my family,
whom always come first in my book

CHAPTER ONE

INDTRODUCTION

1.1. Dielectric Materials

Dielectric materials will not conduct electricity, but will store or carry charges for short ranges under the influence of an externally applied electric field. All solids consist of positive and negative charges, so when an electric field is applied, these charges will separate. This separation of charge is called polarization and can be utilized to store or carry charges over short distances. Piezoelectric materials are a particular type of dielectric material capable of using this separation of charge to convert energy. Most piezoelectric materials are ceramic; however, this research was concentrated on composite piezoelectric materials consisting of a ceramic powder suspended in a polymer matrix.

1.1.1. Polar Effects

Piezoelectricity, pyroelectricity, and ferroelectricity are material characteristics that result from certain crystal structures. Fundamentally, piezoelectric materials become electrically polarized when subjected to stress. As result, they can be used to convert mechanical energy and electrical energy from one form to the other. Pyroelectric materials have a crystal structure that is spontaneously polarizable and is influenced by a change in temperature. Materials with a spontaneously polarizable crystal structure that can be reversed with the application of an electric field, and remain polarized upon the removal of the electric field, are known as ferroelectrics.

1.1.2. History of Piezoelectric Materials

One of these effects, now called pyroelectricity, was first noticed in the early 1700's. Scientists noticed that when tourmaline crystals were initially placed in hot ashes they would attract and repel the ashes.[1] It was not until 1880 that piezoelectricity was discovered. Pierre and Jacques Curie are given credit with the discovery of piezoelectricity when they noted that certain crystals generate a charge on their surfaces when compressed in particular directions. Eventually, the two brothers developed the basics of piezoelectric behavior and documented responses of materials like Rochelle salt, quartz, and topaz.[2] In 1946, Walter Guyton Cady wrote one of the first articles to explain the physics of piezoelectricity. His book, *Piezoelectricity,* provided a core understanding of piezoelectric behavior and led the way for current work.

1.1.3. Crystallographic Classifications

The relationship between piezoelectrics, pyroelectrics, and ferroelectrics is best shown by explaining their crystallographic relationship. All material crystal structures can be classified as belonging to one of 32 point groups. Of these 32 point groups, 11 are centrosymmetric, and thus non-polar crystals. The remaining 21 point groups are non-centrosymmetric; meaning they exhibit no center of symmetry. Of these 21 non-centrosymmetric crystals, 20 of them show a piezoelectric response, meaning that they will demonstrate polarization under an applied field of stress. Of the 20 piezoelectric point groups, 10 have one or more polar axes. These 10 points groups are polar because they have a permanent dipole, but the center of the positive charge does not coincide with the center of the negative charge. These 10 crystals are spontaneously polarizable, with the magnitude of polarization dependent on temperature. A subset of these 10 crystals is

ferroelectric, which show spontaneous reversible polarization and the ability to remain polarized upon the removal of an electric field. Ferroelectrics are reversibly polarized by the application of an electric field. Consequently, all ferroelectric crystals are pyroelectric, and all pyroelectric crystals are piezoelectric, but not vice versa.[3]

Ferroelectricity has been labeled as a subset of piezoelectricity because of some crystals' ability to spontaneously reverse polarization with the application of an electric field and remain polarized upon the removal of the electric field. Ferroelectricity usually vanishes above the materials Curie Temperature T_C. Above this temperature, the material is said to be in a paraelectric state and obeys the Curie-Weiss Law. Below T_C, the material is spontaneously polarizable, and will produce a hysteresis loop when polarization is plotted against applied electric field.[4]

1.1.4. Piezoelectric Effects

Piezoelectric materials have two responses allowing them to convert between mechanical and electrical energy. The primary effect is called the direct effect. This is when a force applied to a piezoelectric crystal produces a charge on the crystal surface. The secondary effect is known as the converse, or indirect effect. This is when the application of a voltage across a piezoelectric crystal results in a shape change. Both the direct and converse effects are commonly used for various devices.

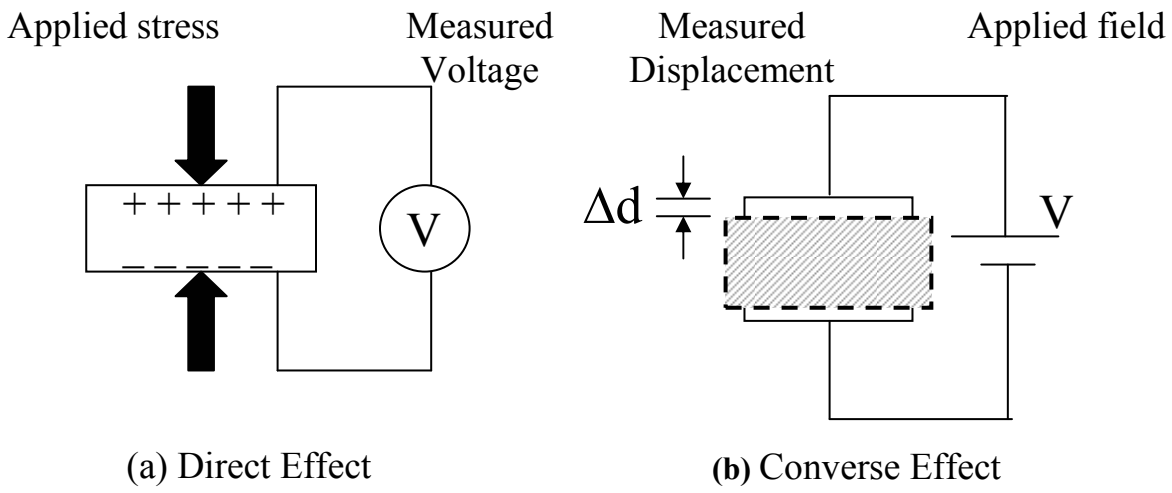

Figure 1.1: A diagram illustrating the direct **(a)** and converse **(b)** piezoelectric effects.

The equations below are the constitutive equations of piezoelectric materials. They describe the two piezoelectric effects with respect to electrical and elastic properties.[5]

<u>*Direct Effect*</u>: $D = dT + \varepsilon E$

<u>*Converse Effect*</u>: $X = sT + dE$

where

D = *charge density*

d = *piezoelectric coefficient*

T = *stress*

ε = *permittivity of the material*

E = *electric field*

X = *strain*

s = *compliance*

D is equal to the surface charge divided by area, d is a piezoelectric coefficient and is discussed in more detail in Appendix A.3. The above equations are commonly represented in a matrix to form a set of equations that can relate properties of a material along various orientations.

1.1.5. Ferroelectricity

As briefly discussed above, a ferroelectric material is a spontaneously polarized material in which polarization can be reversed by applying an electric field. The most commercially developed ferroelectric ceramics are based upon the titania compounds with perovskite structure, such as $BaTiO_3$ and $PbTiO_3$. Ferroelectric materials such as these go through a phase transition from a centrosymmetric non-polar lattice, to a non-centrosymmetric polar lattice at the critical temperature. Most perovskites are cubic at elevated temperatures and become tetragonal at lower temperatures; this is known as the paraelectric to ferroelectric transition. The most notable dielectric change in this transition is a sharp increase in the dielectric constant around the critical temperature.[6] Figure 1.2 shows the phase diagram of $PbZrO_3$ and $PbTiO_3$, two of the most developed perovskite materials.

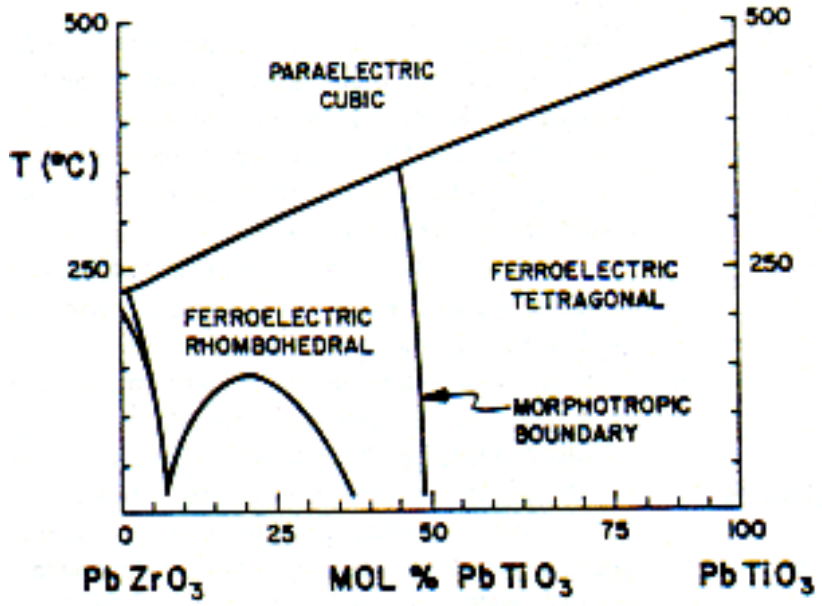

Figure 1.2: A Phase Diagram for $PbZrO_3$ and $PbTiO_3$ showing the influence of composition on crystal structure.

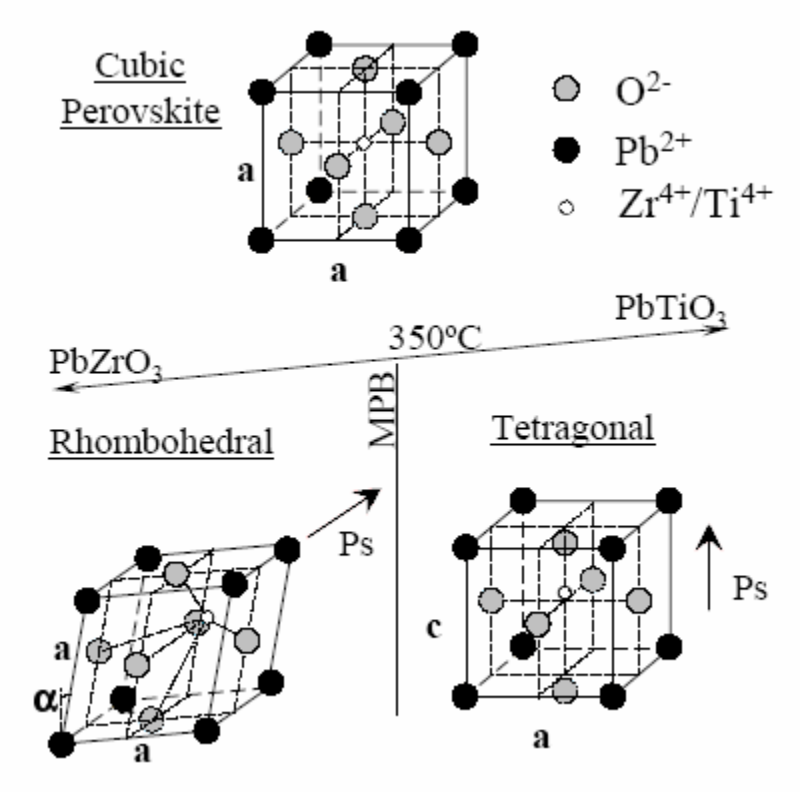

Figure 1.3: A diagram of the perovskite unit cell for lead zirconate titanate $Pb(Zr_x,Ti_{1-x})O_3$ (PZT) showing cubic behavior above T_C as a centrosymmetric cubic structure with zero net polarization, and below the T_C as a non-centrosymmetric tetragonal or rhombohedral structure with a net polarization.

Another important characteristic of ferroelectric materials is called a domain. A domain is a microscopic region of a crystal in which the polarization is homogenous. These domains are naturally un-aligned, but can be aligned in a common direction by applying a DC electric field for an extended period of time. This procedure is called 'poling'.[7]

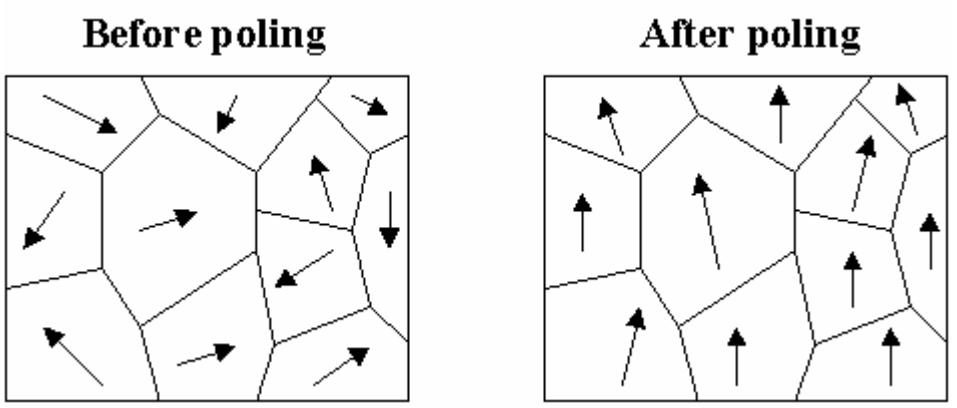

Figure 1.4: A diagram of ferroelectric domain structure before **(a)** and after **(b)** poling. Before poling the domains have random orientation. After poling, there is a remnant polarization P_r along the same direction the field was applied.

Ferroelectric materials are classified as non-linear dielectrics. This means that when an electric field (E) is applied to the material, the stored charge (Q) does not result in a linear response. Figure 1.5 shows this effect with a plot showing a linear and nonlinear response. The non-linear response for ferroelectric materials is called a hysteresis loop. At lower applied fields, the polarization is similar to a linear dielectric and is fully reversible. As the applied field increases to a saturation point (P_{sat}), polarization will remain after the electric field is removed. Polarization saturation (P_{sat}) is the point at which polarization will no longer increase with increasing electric field. The remaining polarization in the dielectric material after the field has been removed is called the remnant polarization (P_{rem}). Remnant polarization is basically a measure of the residual alignment in the domains due to the applied field. The coercive field (E_C) is the

amount of applied electric field needed to return the material to a state of zero polarization. Several factors including composition, thickness, grain size, electrode properties, synthesis route, and residual stress, effect the shape and values of the hysteresis loop.[8] Each of these can have a large influence on the ferroelectric and piezoelectric properties of the resulting material.

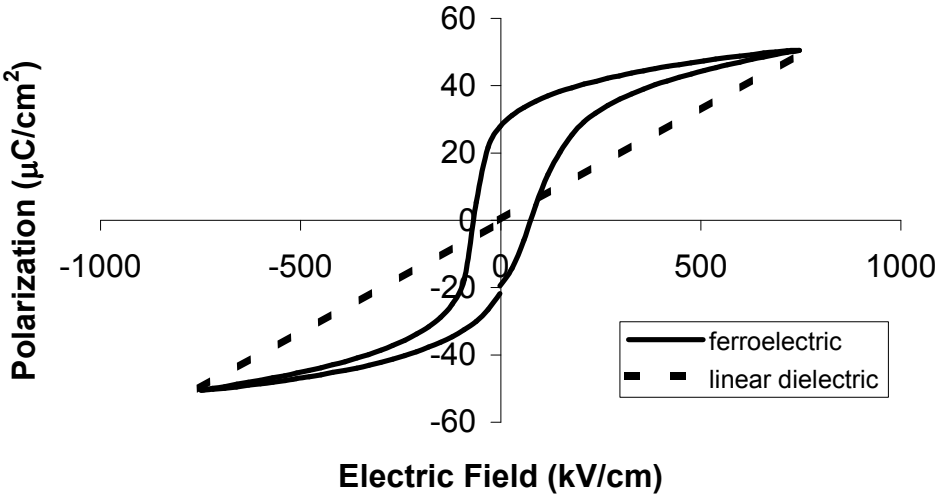

Figure 1.5: An example of a non-linear polarization response from an applied electric field in a ferroelectric material (hysteresis loop), and a linear response of a linear dielectric material.

In order for a ferroelectric material to remain reasonably active it must retain its polarization over time, despite various pressures of degradation. A ferroelectric material must resist degradation due to time, cyclic voltage, and DC bias. Common shortcomings of ferroelectric materials are ferroelectric fatigue, ferroelectric aging, and resistance degradation. Ferroelectric fatigue is a degradation caused by the presence of a cyclic voltage. Ferroelectric aging is a spontaneous change in characteristics measured by

polarization and voltage, noticed after a significant amount of time. Resistance degradation is a decrease in resistance due to a decrease in insulative properties of a dielectric material under DC bias for an extended amount of time.[8]

1.1.6. Applications of Piezoelectrics

Many commercial piezoelectric materials are based on ferroelectric crystals. The first commercially developed piezoelectric material was $BaTiO_3$. However, one of the most widely exploited piezoelectric materials today is $Pb(Ti,Zr)O_3$ or PZT.[3] The main uses of piezoelectric materials are in the detection of mechanical vibrations, generation of charge at high voltages, control of frequency, and generation of acoustic and ultrasonic vibrations. Actual devices utilizing these capabilities are often sensors, actuators, transducers, and generators. Most of these devices are currently produced using bulk ceramics formed into common shapes. Plates, cylinders, washers, and blocks are commonly used for applications such as ultrasonic imaging, underwater hydrophones, thermal imaging, pollutant sensors, inkjet printers, and microphones. Bulk material processing for these common shaped and sized materials has advanced through many years of research, resulting in high quality devices with a good degree of accuracy and precision.[4]

A more cutting edge use of piezoelectric materials is in the fabrication of micro-electrical-mechanical-systems (MEMS). This is a relatively new area of study, based on techniques originally designed for the integrated circuits industry. These techniques are used to fabricate smaller devices that can perform the same function as their bulk material equivalent, at an equivalent or higher level, and at a lower cost. MEMS devices are designed on the micron scale and involve an energy conversion from electrical to

mechanical, or vise versa. The first two mass-produced MEMS devices, appearing in the early 1980's, were an automotive pressure sensor and a disposable blood pressure sensor. A review paper on MEMS technology was first provided by Kurt Peterson in 1982, titled "Silicon as a Mechanical Material". In this paper, Petersen highlighted proposed devices that are still being researched today, such as ink jet nozzles, gas chromatographs, coolers, and pressure transducers.[9] More advanced MEMS devices to be developed in recent times include micro heat engines for electricity generation, micro pumps for drug delivery, and motors for small scale power systems.

Another popular, and modern, use for piezoelectric materials is in ultrasonic medical applications. Much progress has been made in recent years in the area of ultrasonic diagnostic equipment. This is mainly because of advancements in the piezoelectric materials being used as the vibrating material, and of advancements in instrument electronics. Ultrasonic imaging is a superior diagnostic tool because it does not involve surgery or other invasive procedures, it is safer than x-ray imaging, and can distinguish between soft tissues and organs. However, the ability to image soft tissue and organs is only beneficial for particular applications, as is the ability to image bone and cartilage with x-rays for other applications.[10] Ultrasonic imaging and x-ray imaging are more less complementary to each other.

The applications of medical imaging span a wide frequency range of about 1.5-30 MHz, depending on the organs to be imaged. The frequency range is determined by the necessary wavelength needed to attain good resolution. The velocity of sound is 1500 m/s in the human body, and the resolution varies from l mm – 50 μm for a frequency range of 1.5-30 MHz.[27] With higher frequencies, near 30 MHz, better image resolution is

obtained, but only penetrating to a depth of a few millimeters. The relationship between velocity (v), frequency (f), and wavelength (λ) is described in the following equation.

$$v = f \cdot \lambda$$

As a result, the degree of resolution depends on the balance of frequency and wavelength, with the highest frequency producing the highest resolution at shallow distances.
The highest frequency that can be used for a given application is limited by a frequency dependent attenuation within the body, approximately 0.5 dB/cm·MHz for soft tissue.[27] The frequency needed for an ultrasonic application must first be determined for a given wavelength so that the transducer dimensions can be designed to produce resonance at the desired frequency. The resonant frequency of piezoelectric films depends on the thickness of the material and the physical dimensions of the device.

Soft PZT ceramics are widely used as transducers for medical imaging. They have an acoustic impedance of 34 MRayl, which is very high compared to the impedance of soft tissue in the human body of only 1.5 MRayl. Accordingly, there is a reflection of the signal at the transducer / body interface. Losses at the interface are usually minimized by using matching layers with an average impedance of the transducer material and the tissue being examined.[10]

1.1.7. Piezoelectric Composites

Developing a composite material is a common way to tailor material properties for particular applications. Generally speaking, a composite material is considered to be any multiphase material that shows a significant proportion of the properties of both constituent phases, such that a better combination of properties is realized.[30] To modify the mechanical properties of certain piezoelectric materials, some composite materials

have been created. One such ceramic-polymer composite consisting of nanocrystalline lead titanate/vinylidene-trifluoroethylene is discussed by Chen, Chan and Choy. Composites pertaining to this research are discussed in future sections; however, the following information is a brief discussion of composite categorization.

Composite nomenclature refers to a combination of two materials for an overall improvement of properties in the final product. Usually, a composite is composed of two phases; one is called the matrix, which is continuous and surrounds the other phase, the other phase is usually called the dispersed or discrete phase. The properties of the composite are a function of the properties of the constituent phases, their relative amounts, and the geometry of the dispersed phase. Dispersed phase geometry refers to the shape, size, distribution, and orientation of the particles.[18] The numbers used to identify the type of such a material are usually given as a combination, like 0-3. The first number refers to the connectivity of the dispersed phase, the second number is the connectivity of the matrix.

The properties of such a composite depend on the connectivity of the phases, volume percent of ceramic, and the spatial distribution of the active phase in the composite. The concept of connectivity describes the arrangement of the component phases within a composite, which is very important in determining the electromechanical properties of the composite.[18] Figure 1.6 shows ten different types of connectivities possible in composites of two primary materials. In the figure, A refers to the number of directions in which the active phase is self-connected or continuous. B shows the continuity directions of the passive phase. Density, acoustic impedance, dielectric constant and piezoelectric properties like the electromechanical coupling coefficient k_t

change with the volume fraction of the ceramic and polymer, and the type of connectivity.

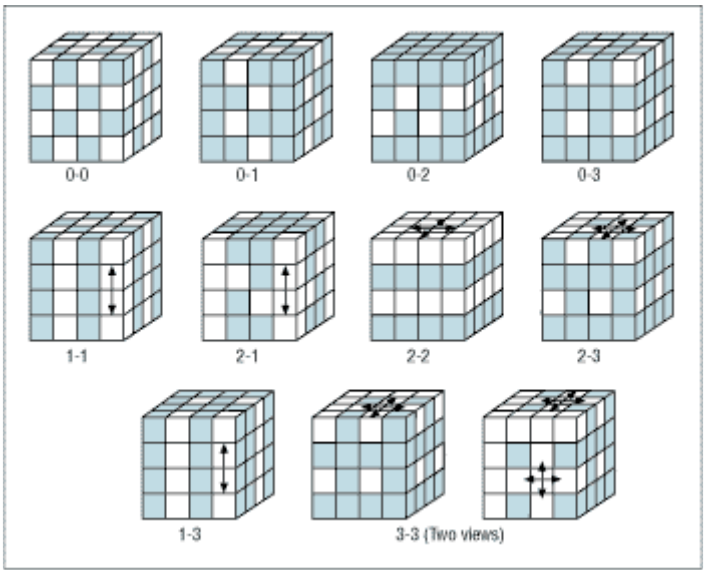

Figure 1.6: Connectivity patterns for a twin phase solid A-B. The shaded parts represent the active phase (A); the white parts show the passive phase (B).

1.2. Piezoelectric Polymers

1.2.1. What Polymers and Why

The existence of piezoelectricity in certain synthetic and biological polymers has been known for a long time; examples of natural piezoelectric polymers are wood and tendon. Interest in these materials was rather small until Kawai and others found that substantial piezoelectric and pyroelectric activity could be generated in synthetic polymer films after being subjected to a strong DC electric field at an elevated temperature. Due to their flexibility and other superior mechanical properties, these materials have opened up possibilities for new applications and devices, and become a subject of interest in the

scientific community. The best known and most commercially active example to date is polyvinylidene fluoride (PVDF).

For technical applications, a polymer with a high piezoelectric response is essential. In order to have high piezoelectric properties it is necessary to form a remnant polarization; coincidently, the few polymers that do form a remnant polarization are also ferroelectric. So far, four polymer families are known to have ferroelectric properties, they are PVDF and its copolymers with trifluoroethylene (TrFE) and tetrafluoroethylene (TFE), the odd numbered nylons, various VDCN (vinylidene cyanide) copolymers and aromatic and aliphatic polyurea. The mechanisms used to stabilize the remnant polarization are quite different in these polymers. The PVDF is stabilized by injected or trapped charges formed at the surface of the crystallites by oriented molecular dipoles. The odd numbered nylons are likely stabilized by hydrogen bonds and the VDCN copolymers may be stabilized by applying a DC electric field (poling) while the material is cooled through the Curie Temperature. Although the Curie Temperature varies for these polymers, PVDF shows the highest piezoelectricity at room temperature, but decreases with increasing temperature. The piezoelectricity of the odd numbered nylons increases above 80˚C and remains unchanged up to the melting point at about 250˚C for Nylon 5. The VDCN copolymers and polyurea show the best piezoelectricity from room temperature to the softening point of about 170˚C.[11]

Because PVDF shows the highest piezoelectric response at room temperature, it has been the most extensively studied material in the last 25 years, while the other three have only had limited interest. Since 1969, when Kawai discovered a presence of piezoelectricity in PVDF, it has been found that strong piezoelectricity exists from

uniaxially drawn polyvinylidene fluoride after it has been poled in a suitable electrical field.[12] The ferroelectric, and thus piezoelectric, properties of PVDF are an example of the interaction of charges and dipoles, charge injection, charge trapping and detrapping, and the influence of different crystal phases on the physical and electrical properties of polymers. PVDF copolymers such a trifluoroethylene (TrFE) have also been studied since the early eighties, with most of these copolymers having strong ferroelectric properties of their own. PVDF-TrFE also shows a reversible transition at the Curie Temperature, from a ferroelectric to a paraelectric phase, with strong dependence of the Curie Temperature depending on chemical composition.[12]

PVDF has also been found to remain ferroelectrically stable after many years of preservation. The plot below shows the surface charge on PVDF samples measured after 22, 27, and 35 years of being wrapped in metal foil and stored in a desicator.[2]

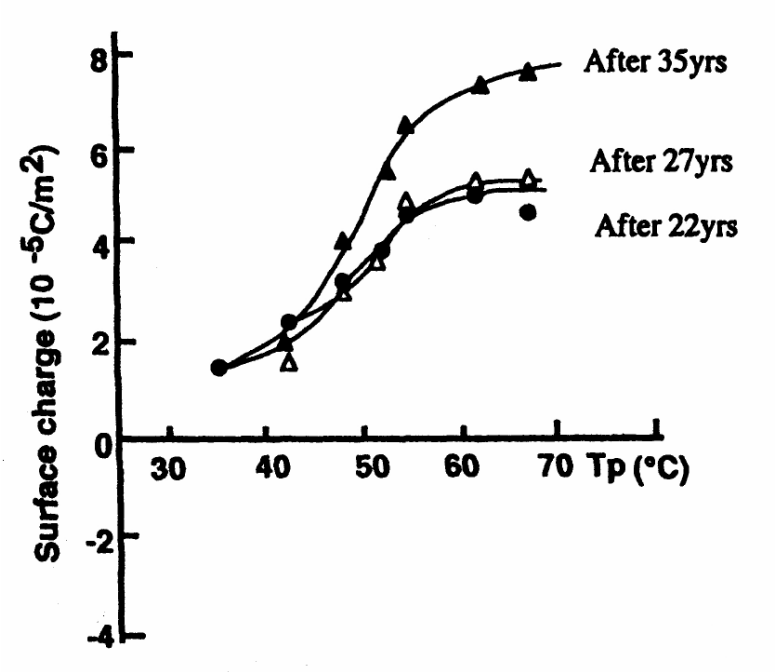

Figure 1.7: A study of surface charge on PVDF samples at 22-35 years after preparation. The magnitude of the surface charge is plotted against the poling temperature with a poling electric field of 4 MV/m.

1.2.2. Polyvinylidene Fluoride and Copolymers as Piezoelectrics

The atomic structure of PVDF is CH_2CF_2. PVDF has been found to have four crystal phases named α, β, γ and δ phases. The crystallinity is about 50 to 60% depending on the amount of chain ordering defects; and the size of the crystallites and chain packing is influenced by annealing. The α phase is the most stable phase at room temperature; therefore PVDF films crystallize into this phase from the melt. The crystallization forms a trans-gauche chain conformation with a unit cell that has two parallel chains. A trans-gauche chain conformation is a "cross-linked, non-planar" chain formation, with two of these chains making up one unit cell of PVDF.[11]

The CH_2CF_2 molecular units in the polymer chains of PVDF have net dipole moments, pointing from the relatively electronegative fluorine atom to the hydrogen atom, and can crystallize in an arrangement having macroscopic polarization. Figure 1.8 A shows the 'all-trans' or TTTT conformation of the polar β phase. The β phase crystallizes into a simulated hexagonal polar packing as shown in figure 1.8 C. Another important crystal phase is the 'trans-gauche' or TGTG conformation shown in figure 1.8 B. This conforms into the paraelectric α phase shown in part D of figure 1.8, and has no net polarization.[13]

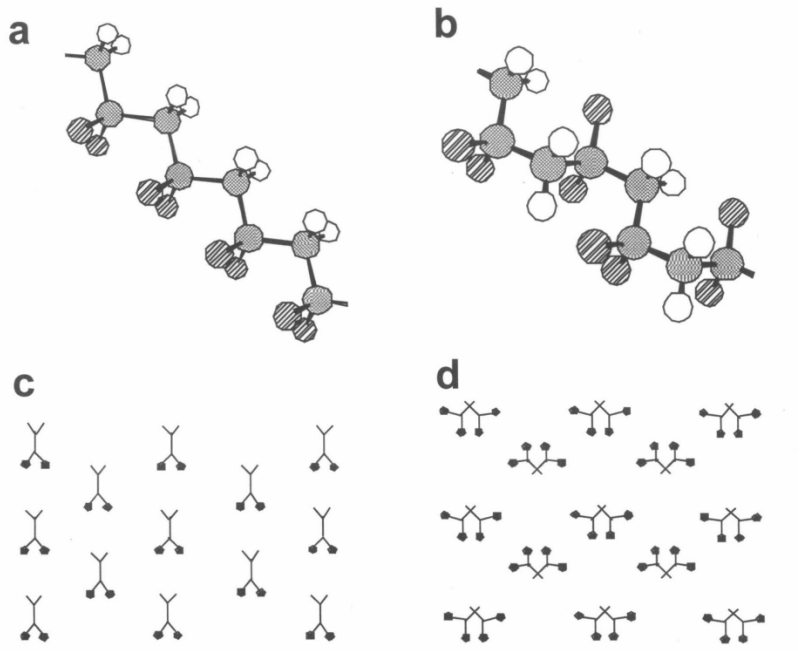

Figure 1.8: Atomic structure of PVDF. Carbon atoms are gray, fluorine atoms are striped, and hydrogen atoms are white. **(A)** is the 'all-trans' conformation of β phase PVDF. **(B)** is the 'trans-gauche' conformation of α phase PVDF. **(C)** is the crystal structure of β phase PVDF, and **(D)** is the crystal structure of the α phase.

The dipole moments of the α crystallites are oriented in opposite directions, resulting in a zero net polarization. The non-polar α phase is transformed into the polar δ phase by applying an electric field greater than, or equal to, 130 MV/m.[28] This electric field rotates every second chain around the molecular chain axis resulting in a parallel orientation of all dipoles in the crystallites, while the chain conformation and unit cell remain the same.

To produce the β phase of PVDF, mechanical stretching of the α-PVDF to about 300% of its original length at temperatures around 100˚C must take place. This causes an overall flip of the molecular chains and produces spontaneous polarization (ferroelectricity) in the crystallites. The β phase of PVDF consists of a simulated hexagonal unit cell with parallel oriented dipole moments. The highest dipole moment of the β phase is perpendicular to the chain axis and is about $7x10^{-30}$ C·m per monomer unit. The β phase of PVDF shows the highest piezoelectric effect of the four crystal phases, but in actual PVDF films there are likely many crystal phases coexisting.[12]

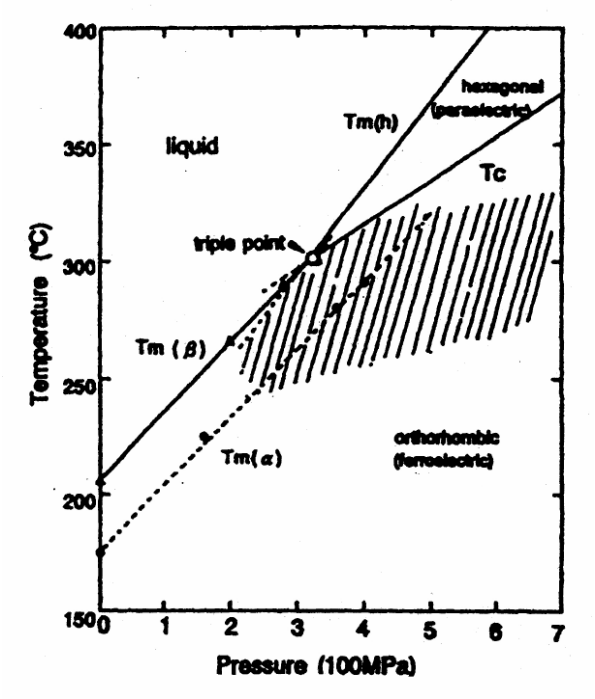

Figure 1.9: P-T Phase Diagram for β phase of PVDF. The melting temperature of the α crystallites is shown by a dotted line. The metastable hexagonal phase appears in the hatched region.

If PVDF is polymerized with TrFE, the result is a copolymer PVDF/TrFE, with randomly distributed monomer units. The extra fluorine atoms in the chain reduce the influence of the head to head and tail to tail defects. This effect increases the crystallinity of the copolymers to about 80%, after the copolymer films have been annealed at 135˚C for at least one hour. If the TrFE content is higher than 18%, then the PVDF/TrFE copolymer will crystallize with the same chain conformation as the β-PVDF. The β phase of this copolymer can be further improved by simultaneous stretching and corona poling. Because of the larger fluorine atoms, the a and b axis of the unit cell of the copolymer are larger than those of β-PVDF, and therefore cause faster dipole alignment

than β-PVDF.[14] The resulting lattice structure and dipole alignment of the copolymer are the same as PVDF. Even though the TrFE monomer unit has a smaller dipole moment than PVDF, the polarization of the copolymers is usually higher than pure PVDF because of the higher crystallinity of the copolymers.

Extensive research to increase crystallinity of PVDF and PVDF/TrFE copolymers has been performed over the last few years. It is believed that higher crystallinity will provide higher piezoelectric properties. Ordinary, crystallization of these polymers results in folded chain crystals (FCC), however, if the polymers are crystallized in the hexagonal paraelectric phase, they will form extended chain crystals (ECC). The ECC have a greater distance between the chain foldings than the FCC, and show a higher electromechanical coupling factor, but studies have found that the hexagonal paraelectric phase for PVDF exists only under high temperature and high-pressure conditions. PVDF films produced by this method show the highest electromechanical coupling factor ever found for PVDF, and have an increased melting point, increased sound velocity, and an improved thermal stability of piezoelectricity up to the melting temperature of 205˚C. For PVDF/TrFE copolymers the ECC can be formed by crystallization at atmospheric pressure. It has also been discovered that the size of the crystalline domains can be greatly increased if the crystallization takes place with no constraints other than the tensile stress along the chain axis.[26] Films processed this way show an increased electromechanical coupling factor and a very anisotropic sound velocity.

Another way to form highly oriented PVDF copolymer structures is vacuum evaporation of the polymer on suitable substrates. Of course the total thickness, substrate temperature, deposition rate, application of an electric field, and the substrate type and

material strongly influence the alignment of the polymer on the substrate. Strong alignment of polymer chains can also be produced by the Polymer Induced Alignment technique. This is where the polymer chains are produced by evaporation on glass with an intermediate layer of highly oriented PTFE.[15]

Not only are the oriented dipoles in the crystallites important to the stability of the remnant polarization in PVDF, but also the effects of trapped charges. Experiments have found that a decrease in conductivity of PVDF with increasing pressure indicates ionic charge transport. Further experiments found that charges could be injected and trapped with blocking electrodes. In this process, electrons are injected from the cathode into the PVDF film, causing F- ions to split off from the chains by electrochemical reactions. At the anode, holes are injected and the H+ ions are formed. These ions then serve as charge carriers for the conduction process and for polarization stabilization by charge trapping. Some of the ions also recombine to hydrogen fluoride, which is emitted by the polymer film.[11]

Poled polymer films show tensile, thickness and shear piezoelectricity similar to piezoelectric ceramics. It is clear that the lasting polarization produced in polymers consist of both oriented dipoles and trapped charges, with the dipoles aligned normal to the surface of the film by poling. Dipoles are oriented in the crystalline phase inside the lamellae and also in the interfaces between the crystalline and non-crystalline phases where molecules are aligned in parallel. The ions and electrons that were either injected from electrodes or originally present in the polymer remain trapped in the polymer.[11] The most common theories explaining the origin of piezoelectricity of poled polymers are the dimensional effect and the intrinsic effect.

The dimensional effect is basically explained as follows. If the residual polarization caused by the oriented dipoles or trapped charges is unchanged, the lateral stretching reduces the thickness of the film, which increases the induced charge in the electrodes.[16] According to this theory, the piezoelectric constant e_{31} (polarization P_3/strain ε_1) is the product of Poisson's Ratio ν_{31} times the residual polarization Pr.

$$e_{31} = (P_3 / \varepsilon_1) = \nu_{31}(P_r)$$

In more detail, this means that the piezoelectric constant e_{31} is equal to the polarization through the thickness of the film divided by the strain as a result of stretching in the machine direction. This is also equal to the strain in the transverse direction divided by the strain in the thickness direction (Poisson's Ratio), times the residual polarization.

The intrinsic effect is explained similar to the following. The residual polarization is changed by the applied stress on the crystalline phase, which includes the oriented molecules in the non-crystalline phase. This intrinsic effect is determined by the product of the electrostriction constant times the residual polarization Pr.[16] The electrostriction constant relates a materials deformation to an applied electric field.

The piezoelectric interest of PVDF is based on the various applications and on the fact that the existence of ferroelectricity in this material is an example of the interaction of charges and dipoles, charge injection, charge trapping and detrapping and the influence of different crystal phases on the physical and electrical properties of polymers. PVDF has been the most extensively studied piezoelectric polymer for these exact reasons, and has also found many new and increasingly more applications that piezoelectric ceramics cannot fulfill. Unfortunately, the piezoelectric properties of polymers like PVDF and its copolymers are small in comparison to piezoelectric ceramics. This issue has generated

much research in improving and developing better piezoelectrically active polymers and compliant materials.

1.2.3. Research Objectives

From the great wealth of research on ferroelectric materials, it is clear that ceramic materials are superior in piezoelectric properties. The only other piezoelectric materials known are semi-crystalline polymers like PVDF and vinylidene cyanide (VDCN). It is also apparent that copolymers such as trifluoroethylene and tetrafluoroethylene help to improve the piezoelectric response in PVDF by improving the crystallinity. Further improvements in piezoelectric properties may be achieved by developing a 0-3 composite material with a highly piezoelectric ceramic, such as lead zirconate titanate (PZT), and a piezoelectric polymer like PVDF.

Naturally, ferroelectric, pyroelectric, and piezoelectric ceramic materials are excellent candidates for use in solid-state applications like transducers and micro-electrical-mechanical devices. However, two limiting factors of ferroelectric ceramics are the high stiffness and inability to conform to softer materials, and the relatively higher cost of fabrication. These are the primary reasons that piezoelectric polymers have been studied so extensively. Piezoelectric polymers are very flexible, easy to fabricate, and have an acoustic impedance comparable to soft human tissue.

Another interesting benefit of a soft, flexible piezoelectric material is in medicine. Electrical, magnetic, ultrasonic, and piezoelectric stimulation of soft tissue wounds has been shown to increase fluid flow, and therefore promote healing. One hypothesis is that a therapeutic transducer can be developed to stimulate the healing of tissue wounds via piezoelectric response. This transducer would be a ‘band-aid-type’ transducer with an

acoustic impedance matching that of soft human tissue. Piezoelectric polymers would be ideal for such an application because of their flexibility and ease of fabrication. Piezoelectric polymers are easily processed to different shapes, making them ideal for various applications on the body. They are also relatively low cost, and could be designed for disposable applications, making them perfect for temporary use in the medical industry.

Other research has shown that bone and tendon are slightly piezoelectric. This has lead to further exploring of the stress-generated potential in bone, and the resulting fluid flow in the structure of the bone. Similar to the theory of using a piezoelectric response to stimulate healing in soft tissue wounds, the field of orthopedics has gained a strong interest in the piezoelectric stimulation of bone fractures. Several clinical devices have been developed to stimulate bone growth and fracture healing by increasing the fluid flow with ultrasonic and piezoelectric input.[10] One limiting factor of such devices is that in order to produce enough piezoelectric stimulation, a piezoelectrically active ceramic material must be used. This results in a very rigid device that is not easily adapted to the body. A flexible transducer capable of producing a high piezoelectric response would be ideal for such an application. This is not likely possible with piezoelectric polymers alone, but may be possible with certain polymer-ceramic composites.

Piezoelectric polymers have many desirable properties over piezoelectric ceramics. Most prominently, are the mechanical properties of piezoelectric polymers over ceramics. Ceramic materials are hard and brittle, and require more complex production than polymers. Although ceramics are ideal for some piezoelectric

applications, a flexible and highly piezoelectric material would be far more applicable for many devices. Ultimately, a material with the mechanical properties of a polymer like PVDF, and the piezoelectric properties of a ceramic like PZT, would be ideal for almost any piezoelectric application at or around atmospheric temperature. The goals of this research project are based on these ideas, and the applications of such a material.

PVDF based piezoelectric polymers and copolymers that are capable of high electric fields, high source levels, and broadband and conformal shapes have permitted their use in a wide range of applications for transducers, actuators, and sensors. The density of these polymers is also very close to that of water and the human body tissues, hence there is no acoustic impedance mismatch with the body. Other advantages of PVDF based piezoelectric polymers and copolymers are flexibility, high mechanical resistance, dimensional stability, homogeneous piezoelectric activity with the plane of the sample, no aging effects up to temperatures of 80°C (PVDF) or 110°C (PVDF/TrFE), chemical inertness, and low acoustic impedance. Unfortunately, all piezoelectric polymers also suffer from high dielectric losses with low a dielectric constant.[17] This results in poor piezoelectric properties, and unavoidably limits their uses as piezoelectric materials. The main goal of this research is to develop a 0-3 type piezoelectric ceramic-polymer composite, with strong improvements on piezoelectric properties, that can be used for flexible transducer applications.

For this research, the 0-3 type composites referred to are ceramic-polymer composites, with the connectivity of the ceramic in zero dimensions, and the connectivity of the polymer matrix in three dimensions. The original proposal was to use a piezoelectric ceramic powder to improve the electromechanical properties of PVDF,

while maintaining the flexibility of the polymer. In such a 0-3 composite, the PZT will be a discrete powder within the polymer matrix.

Primary objectives of this project are:

A) to develop the processing science necessary to incorporate the ceramic powders uniformly into the polymers without losing the flexibility of the base polymer.
B) characterize the composites in order to understand the influence of the piezoelectric ceramic powders on the electromechanical properties of the composites
C) fabricate a simple, and reproducible, low-cost transducer capable of being applied to various devices

The preliminary study involved characterizing the base polymer and copolymer by measuring d_{33}, dielectric constant and dielectric loss. The next part of this research was to develop the processing science needed to create a 0-3 composite. Once the composites have been produced, the influence of the ceramic powder will be evaluated by testing d_{33}, dielectric constant and dielectric loss. Important issues to explore are the influence of solids loading on the piezoelectric properties, reproducibility of results, and reliability of the final product.[19]

Essentially, the use of ferroelectrics is based on two major components; the peak polarization, and the ability to hold a remnant polarization. If these two properties can be improved, a 0-3 composite like this can be applied to several areas of piezoelectric applications. A flexible piezoelectric composite could be applied to all kinds of

transducers, actuators, and sensors that are currently produced with piezoelectric ceramics. Flexible composite piezoelectric materials could also be used for ultrasonic sensors. Having a flexible piezoelectric material capable of sending and receiving ultrasonic signals would be a great development because of the various applications and benefits of such a material. A compliant imaging device would be much more comfortable and produce better ultrasonic images for the medical industry. A compliant film embedded into another composite material or structure could also be used to measure stress and strain, without affecting the overall mechanical properties of the material.

The following chapters explain, in greater detail, the development and characterization of a 0-3 type piezoelectric ceramic-polymer composite based on PVDF/TrFE and PZT. Chapter two consists of two sections explaining experimental design and methodology. The first section is on research of bulk polymer and composite samples. The second section discusses research done on film samples. Following this chapter, is a chapter discussing results and conclusions for both the bulk and film sample experiments. This chapter also includes a final conclusion with recommendations for future work. Next is a short summary of critical developments, followed by an appendix on characterization theory and guidelines.

CHAPTER TWO

RESEARCH DESIGN AND METHODOLOGY

2.1. Bulk Samples

2.1.1. Processing Bulk Piezoelectric Polymers and Composites

The focus of this research has been to develop 0-3 composites of piezoelectric ceramic and polymer materials for flexible transducer applications. It is thought that the high piezoelectric properties of the ceramic material will improve the overall piezoelectric properties of the composite. The primary piezoelectric polymer used in this research is Polyvinylidene Fluoride (PVDF). To remain flexible, these composite samples are a majority polymer by volume, with commercial lead zirconate titanate (PZT) powder suspended in the polymer material.

Research began with the assumption that any thickness of sample could be scaled down to a required thickness. Originally, we focused on production of a bulk sample around one millimeter thick. This seemed like a reasonable thickness that could be developed and tested in our labs, and would be applicable for certain devices we had in mind. The objective was then to make a bulk sample that was solid and uniform, with a thickness of about one millimeter. A basic control sample of PVDF would be needed, as well as various copolymer samples and ceramic-polymer compositions to study. Clearly, we would begin with a bulk sample of pure PVDF. We also planned to test a copolymer of PVDF and Trifluorethylene (TrFE), and a 0-3 Composite of PZT with both the homopolymer PVDF, and the copolymer PVDF/TrFE.

The materials used for these samples were commercially purchased from outside the university. PVDF is in the form of a fine white powder that is pressed into a homogenous sample. The copolymer of PVDF/TrFE is in a 50/50 mixture pellet form, which can also be transformed into a solid sample. The PZT powder is simply a powder that is suspended in three dimensions within the polymer matrix.

To fabricate a homogeneous bulk sample the commercial PVDF powder needed to be transformed into a solid sample. Initially, we thought the powder could be dissolved into a solution, which could then be cast and annealed into a solid sample. After researching possible solvents, we found that PVDF is very chemically stable. Methyl Ethyl Ketone (MEK) was used in other similar research work to dissolve PVDF, so this was attempted. MEK did not dissolve the polymer well enough to produce a solid bulk sample; so many more experiments with various solvents were tried. Further literature review gave several possible solvents for PVDF, but none worked successfully in our experiments. Producing a solid bulk sample was obviously critical to moving forward with research. Eventually, we found that if the polymer powder was heated slightly above the melting temperature, it would melt into a solid bulk sample.

We began making bulk samples in an open container by simply melting the powder into the desired shape. This process made solid polymer samples from the original powder, but with a very irregular thickness and consistency. There was also a large problem with air bubbles forming in the samples while the powder melted. To remove the gas bubbles, we tried melting the polymer powder in a vacuum oven at 200°C on the highest vacuum setting of 25 in Hg. Even at the highest temperature we could use

without burning the powder, the melted polymer remained too viscous for the bubbles to escape.

In order to contain the polymer and produce a dense, uniform sample we decided to use a hot pressing operation. This would require a mold that could be heated while pressing the polymer material into the mold. A hot pressing operation will melt the powder while forming the sample into a uniform shape and pressing the air bubbles out of the material. For ease of cleanup, we made a stainless steel mold that could be pressed between the two hot plates on our press.

Figure 2.1: The hot press used to press samples into a stainless steel mold.

The PVDF powder was pressed into the stainless steel mold at about 180°C (PVDF melts at 175°C). Using the right technique, the samples came out very uniform, with no air bubbles. The samples were a tough and flexible polymer material that could be pressed to various thicknesses depending on the depth of the mold. We have pressed samples ranging from 25 μm to 3.0 mm, but initially focused on samples with a material thickness of 500 μm. The width and length of pressed samples depends on the size of the mold; our standard size is 1.5 cm wide by 5.0 cm long. Finished polymer samples can then be cut with scissors to any size or shape.

This hot pressing process works well to produce bulk samples, as long as a mold release, like silicone lubricant, is used. Without using silicone lubricant, the samples will bond to the metallic mold and burn along the outer surfaces. PVDF also strongly adheres to any metallic surface, including stainless steel. This causes many samples to be destroyed while being removed from the mold, unless a moderate amount of lubricant is used. We eventually found that lining the mold with aluminum foil sprayed with a film of silicone spray would provide the best part release and eliminate the need to clean the mold.

The process for hot pressing polymer samples is as follows:

1. Measure the material (about 3 grams for PVDF, in the 1.5 x 5.0 x 0.5 cm mold)
2. Arrange molds and line with foil
3. Spray with silicone spray

4. With the mold on the bottom plate at approximately 180˚C, slowly pour the powder into the mold

5. Pack powder as it begins to melt to remove pores

6. After material has completely melted, apply mold cover and close press

7. Press the sample at 500 PSI

8. Immediately begin cooling the plates

9. At about 165˚C increase pressure to 1000 PSI

10. Once temperature is under 125˚C, release pressure

11. Remove sample and foil lining

12. Peel foil away from polymer sample

This process successfully produced solid bulk samples of the homopolymer, with no electrodes. The same process is also used to produce copolymer samples from the pellet form copolymer of PVDF and TrFE. The copolymer samples are made from a commercial 50/50 mix of PVDF and Trifluorethylene (TrFE). The exact same process is used for the copolymer samples, including the amount of material used (3 grams).

Composite samples of PVDF/PZT and PVDF/TrFE/PZT have also been produced using the hot pressing method. Before pressing these samples, the composite material must be formed by high shear mixing of the respective powders in a Torque Rheometer at about 200°C. The Rheomix thoroughly mixes the PZT and polymer materials at an RPM of 100 for 1 hour. The batch volume for the composite is approximately 70% of the maximum volume capable of being mixed in this Torque Rheometer. This results in a batch size of 50 cc. The polymer material is the primary material, so it is added first so

that it can melt before the ceramic powder is added. No other additives are used in the composite mixture, only PZT and the respective polymer. Compositions of 75/25 polymer/ceramic by volume have been made using this process for both PVDF/PZT and PVDF/TrFE/PZT samples. Other compositions have been mixed including 85/15 polymer/ceramic and 65/35 polymer/ceramic, but no further processing was done on these materials. It is assumed that any composition can be mixed with at least 60% polymer composition and still retain similar mechanical properties as the base polymer.

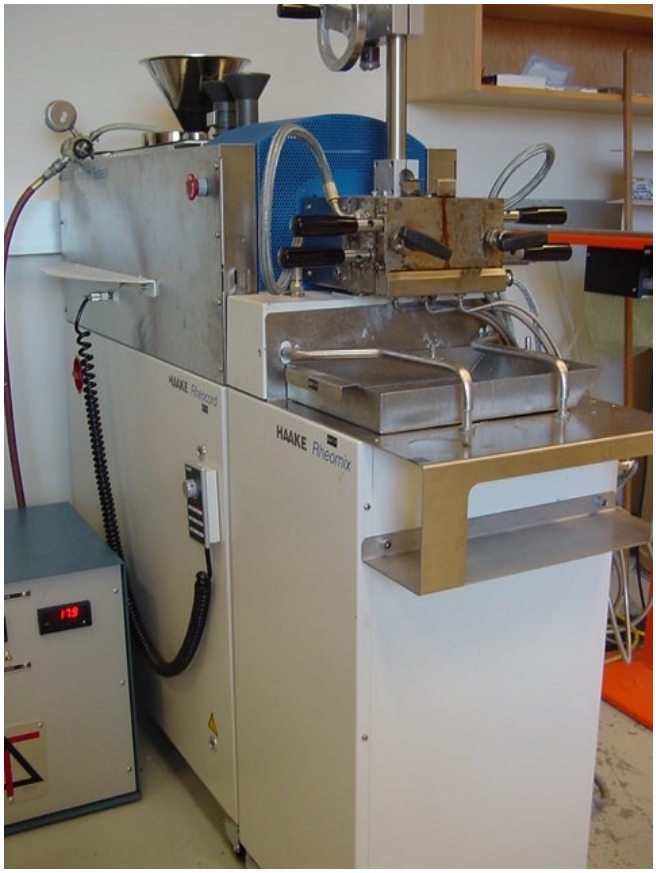

Figure 2.2: A picture of the Torque Rheometer used to mix composite material.

Interestingly, a 75/25 percent polymer/ceramic by volume composite is a 40/60 percent polymer/ceramic composite by weight. This is obviously due to the differences in density between the two materials. The density of PVDF and its copolymer with TrFE is 1.78 g/cc. The density of PZT is 7.85 g/cc. These composite materials remain tough and flexible, with a melting temperature close to 175°C. Overall, the mechanical properties seem to be similar to the polymer materials, except that the density of the composite is significantly higher.

Once the composite material was mixed with the Torque Rheometer, it was removed in bulk globs. The globs were further refined in size by cutting and grinding so that they too could be used in the hot pressing process. The resulting composite material was then used in the hot pressing process, similar to the polymer materials, to produce a solid and uniform bulk sample.

We wanted the β phase for piezoelectric applications, so the PVDF samples required stretching to transform the grain structure from the α phase to the β phase. The copolymer and composite material with TrFE in it should crystallize directly into the β phase, or very closely to it, so stretching or pressing these samples is not necessary. Although it had not been documented, we assumed that pressing or rolling the sample would provide the transformation from the α phase to the β phase. Because of available equipment, and the fact that rolling or pressing the sample would be easier than stretching it, we decided to press the sample biaxially at about 150˚C on the hot press. We also tried rolling the samples with a steel roll at room temperature to deform them uniaxially.

Figure 2.3: A figure of the steel roller used to roll polymer and composite samples. Rolling the sample deforms the material uniaxially in the machine, or length, direction.

Once the samples were rolled or pressed, they needed to be electroded. Originally we tried to use Colloidal Silver Paint as an electrode, but found that it did not bond well with the polymer, and eventually chipped off. Because PVDF strongly bonds to any metallic surfaces, including stainless steel, we decided to line the hot pressing mold with copper foil that could be left on the sample and ultimately act as an electrode. This was just a simple change in the hot pressing process, where we used copper foil instead of aluminum foil, and did not use silicone lubricant on the surfaces of the foil that would be in contact with the polymer. Silicone lubricant was still necessary on the sides of the

mold for mold release, but was not used in the areas where the electrode would be applied. Attention was needed so that silicone lubricant was only applied on the sides of the mold, while keeping the copper foil clean and free of oils so that the foil would bond well. To provide the best adhesion between the copper foil and the polymer, the copper foil sheets were wiped with acetone to remove oils before the polymer was added to the mold. This worked quite well and resulted in a uniform, well-bonded electrode using no adhesives. The copper foil used was 25 μm thick.

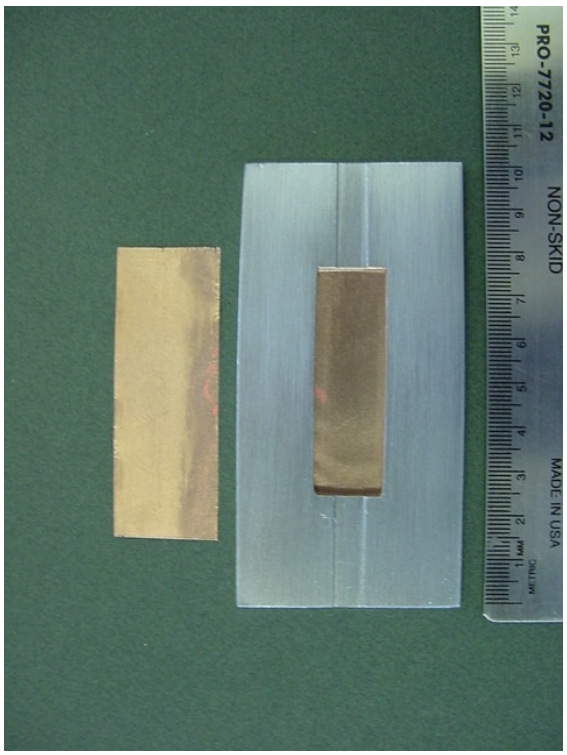

Figure 2.4: A picture of the 3mm thick sample mold, with copper foil sheets that will act as electrodes on the final sample. The bottom electrode is obviously under the mold, the foil sheet on the left will be added to the top, to act as the top electrode, after the mold is filled. Notice the 500 μm deep vents on each end of the mold for gas escape during the pressing process.

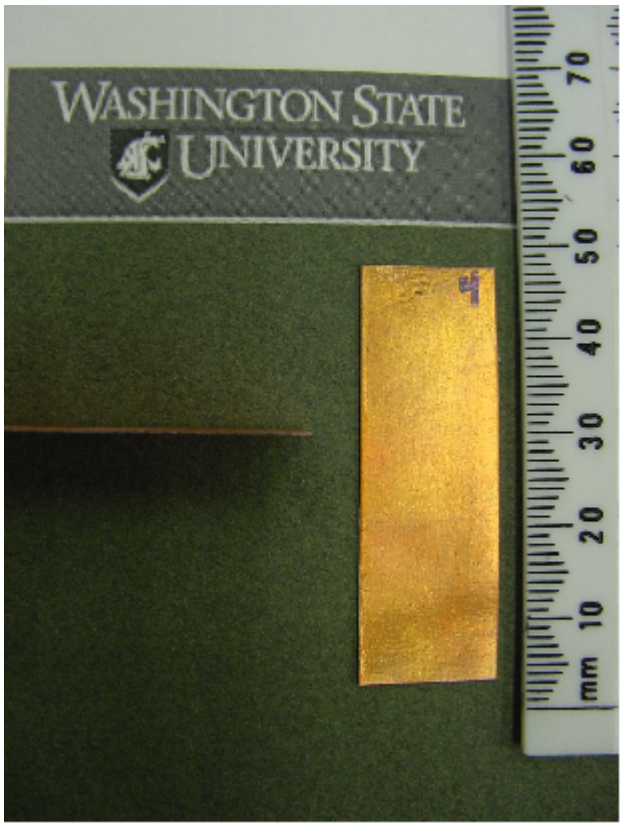

Figure 2.5: The picture above is of two finished 500 μm thick copolymer samples with 25 μm thick copper foil electrodes.

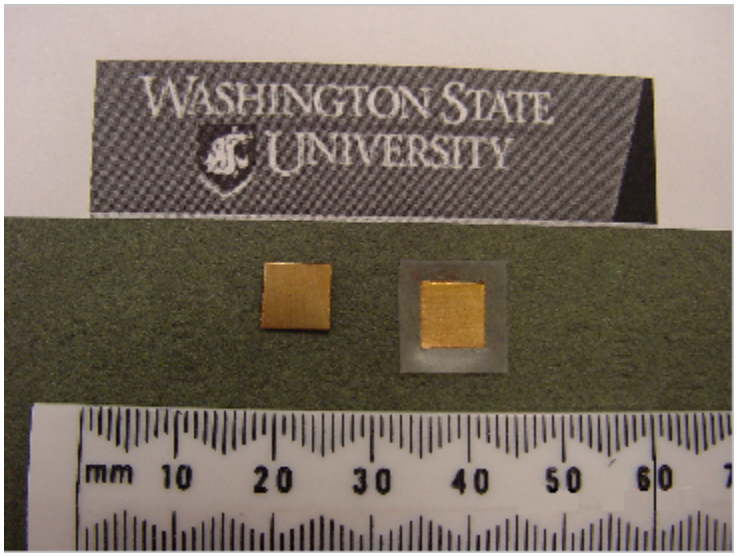

Figure: 2.6: Two finished 1 cm square copolymer samples. The copper foil electrode on the right sample has been trimmed to prevent arcing during the poling process.

2.1.2. Characterization of Bulk Samples

Once we have produced an electroded sample we must pole the material. From other's extensive research on the poling behavior of PVDF it has been found that an electric field of at least 20 kV/mm must be applied to orient the dipoles and produce piezoelectric properties in the material. As a result, a sample 0.5 mm thick would require

an electric field of at least 10 kV for poling. Our DC power supply was able to supply up to 10 kV before shorting through or around the sample. This resulted in a 20 kV/mm poling field on a 500 μm thick sample, which was the minimum amount needed. We tested 500 μm thick samples poled at this voltage, but have been very limited with testing equipment. Due to the high electric field needed to make these bulk PVDF samples piezoelectrically active, we found minimal or no piezoelectric properties while testing for hysteresis and impedance. To increase the applied poling field we have decreased the thickness of the samples to about 100 μm. The d_{33} of a 100 μm thick sample of 75% PVDF/TrFE and 25% PZT is 67 pC/N at 200Hz. No further testing has been done on the 100 μm thick samples because of the errors caused by the small material thickness in relation to lab equipment operating range, and the inability to pole the samples in a higher electric field.

The next step was to make samples in the range of 20 μm to 30 μm so that we could overcome problems with thickness in relation to lab equipment testing ranges. With a material thickness in this range, we can apply about a 40 kV/mm field on a 25 μm thick sample with 10 kV from the power supply. The hot pressing process was again used to produce thinner samples, while using the same electroding procedure. This produced samples that were thinner than the electrode material, which limited the piezoelectric performance of the sample. The modulus of elasticity of the copper foil electrode was a great deal higher than that of the polymer sample, thus limiting any mechanical performance.

2.1.3. Discussion

The conclusion was that film thickness was in the proper range for poling and testing, but different electrodes were needed. Having copper foil electrodes in the nanometer range is not viable. The next best option was to electrode the samples by sputtering gold on the surface. This would produce electrodes of the appropriate thickness, but would require the samples to be made without copper foil electrodes. To produce samples of this thickness, without copper foil electrodes as backing, would be impossible using the hot pressing process. The best way to produce a sample of this thickness would be to spin coat a solution of the polymer or composite material onto a silicon wafer. This would produce a uniform thickness sample without the electrodes, but would call for us to find a solvent capable of dissolving the base polymers.

2.2. Film Samples

2.2.1. Processing of Piezoelectric Polymer and Composite Films

Although bulk samples were not feasible with the given lab equipment, our objective remained the same. The primary goal of this research was to develop a 0-3 composite of piezoelectric ceramic and polymer materials for flexible transducer applications. Obviously, a thinner sample was needed in order to characterize the material with our lab equipment. Much research has been done in the area of piezoelectric film production and micro-electrical mechanical systems. This research can also be applied to thick polymer film samples as needed for our research.

To make thick polymer films, the base materials must be dissolved into a solution or gel that can be spin coated onto a substrate. The typical substrate for this process is a silicon wafer. As discussed earlier, PVDF is a very chemically stable material, commonly used to line pipes and tanks in harsh environments. Although many solvents were unsuccessfully tried in the early stages of research, we began searching again for a solvent to dissolve the polymer material. Eventually, we found that Toluene, DMSO, and Tetrahydrofuran (THF) should dissolve PVDF.[25] Toluene and DMSO temporarily dissolved the polymer powder, but the powder would eventually settle out of solution. THF in a ratio of about 20% material to 80% solvent (by volume) constantly stirred at room temperature, or slightly above, was found to dissolve the material into a gel viscous enough to spin coat onto silicon wafers. Twenty-four experiments were done to find the approximate solutions desired for spin coating each of the three materials onto the silicone wafers. Variables in creating the correct solution include the amount of material (homopolymer, copolymer, or composite), the amount of solvent, and the mixing time and conditions, such as temperature and stir rate. The best mixing conditions for all three materials seemed to be at about 30°C, for 30 minutes with aggressive stirring and the beaker covered. For the homopolymer and composite, a solution with 1.5 grams of solid material to 10 mL of THF was used. The copolymer material was in pellet form, so required a slightly different combination. For the copolymer, 3 grams of pellets were combined with 15 mL of THF. Although solution viscosity and dissolution can be modified by changing the solution measurements, this has become the standard solution for each of the respective materials.

In the spin coating process, the polymer dissolved solution was applied to a silicon wafer spun at a wide range of revolutions per minute. The solution in this research was thin enough to apply through a large syringe. Drops of the solution were placed in the center of the silicon wafer so that they would disperse in a concentrical pattern towards the outside edge of the wafer during spinning. This provided a thin uniform layer of the solution across the surface of the wafer.

The thickness can be directly controlled by several variables. The first of which is solution viscosity; this was controlled by either increasing or decreasing the amount of material, or the amount of solvent used. With less solvent and more powder material, the viscosity of the solution increased and resulted in a thicker film sample. The amount of time the solution was stirred, and whether or not it was heated and covered, also affected the viscosity of the solution. THF boils at approximately 66°C, so the viscosity increased if the solvent was allowed to evaporate for an extended period of time. The second principal way of controlling film thickness was by varying spin rate. The RPM of the spin coating machine can be varied a great deal, which directly affected the thickness of the film. As RPM increased, film thickness decreased as a result of centrifugal force acting on the solution. For simplicity, we chose to keep the solution viscosity constant, and control sample thickness by varying the RPM of the spin coating machine. Forty-two experiments studying solution parameters and spinning conditions have been made to create a table of spin rate and the resulting thickness and dispersion of the sol-gel. This information is given in Appendix C, and has allowed us to create a required thickness for a particular sample each time that we make a sol-gel. The most consistent and highest quality samples are:

15 μm homopolymer sample spun at 2000 RPM for 45 seconds

25 μm copolymer sample spun at 2000 RPM for 45seconds

20 μm composite sample spun at 600 RPM for 45 seconds

Figure 2.7: A picture of the spin coating machine. The silicon wafer is placed in the center of the machine on a spindle, and held in place with vacuum through the spindle.

After the film samples have been spun, they were annealed in the fume hood for several minutes before being placed in storage containers. The annealing was done at room temperature, even though the boiling point of THF is 66°C. At room temperature, the samples transform into a solid uniform film within minutes of ventilation in the fume hood. The annealed samples were bonded to the silicon wafers, which can act as a bottom electrode. If the silicon wafer has a platinumized surface, this surface can be used as a bottom electrode on the finished sample. The next step was to apply a top electrode to the film samples. This was done by masking the desired electrode pattern and then sputtering gold on the top surface. The top electrode for these samples is a simple pattern of dots, one millimeter in diameter. Electrode thickness is 150 nm.

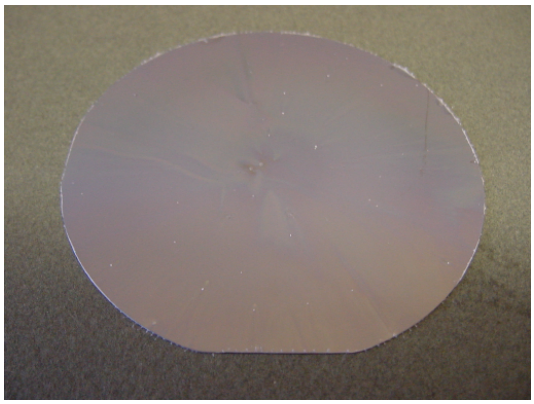

Figure 2.8: A finished homopolymer film approximately15 μm thick on a platinumized silicon wafer.

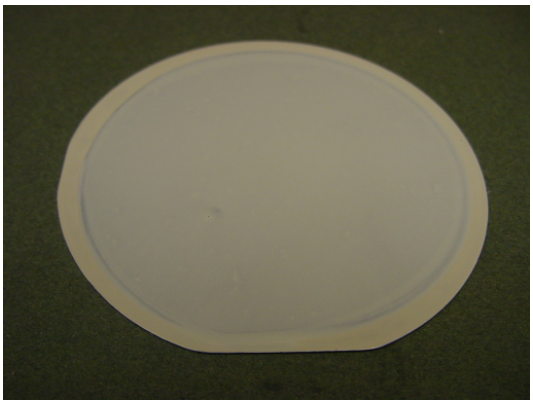

Figure 2.9: A composite film showing the resulting 'ring' of excessive thickness when the sample is spun too fast.

2.2.2. Characterization and Discussion of Prototype Film Samples

After electroding the sample, the films were poled using a corona poling station. This is an enclosed apparatus designed to create an electric field between the tips of several conductive needles and a copper base. The samples were poled in a range of different electric fields, spanning from 20 MV/m as a minimum, up to 80 MV/m. Time for poling has ranged from fifteen minutes up to two hours and thirty minutes. To find the optimal time and electric field for corona poling, several samples were poled for increasing times from fifteen minutes to sixty minutes, and increasing electric fields of 20, 40, 60, and 80 MV/m. The samples were then tested for leakage and peak polarization to identify the best parameters for poling. Poling the samples for fifteen to thirty minutes at 80 MV/m seemed to produce the highest peak and remnant polarization.

Figure 2.10: The Corona Poling Station. This is connected to a DC power supply to create an electrical field between the steel needles and the bottom copper plate necessary for poling.

15 um thick
PVDF Samples

Poling Field (MV/m)	Time (min)	Leakage (nA)	Peak Polarization (uC/cm2)
20	15	0.099	0.011
40	15	0.131	0.026
60	15	0.165	0.035
80	15	0.196	0.041
80	30	0.187	0.045
80	45	0.193	0.044
80	60	0.198	0.045

25 um thick
PVDF/TrFE Samples

Poling Field (MV/m)	Time (min)	Leakage (nA)	Peak Polarization (uC/cm2)
20	15	0.073	0.014
40	15	0.106	0.034
60	15	0.143	0.043
80	15	0.173	0.053
80	30	0.176	0.059
80	45	0.166	0.055
80	60	0.179	0.053

20 um Thick
PVDF/TrFE/PZT Samples

Poling Field (MV/m)	Time (min)	Leakage (nA)	Peak Polarization (uC/cm2)
20	15	0.091	0.018
40	15	0.121	0.039
60	15	0.149	0.058
80	15	0.182	0.076
80	30	0.179	0.077
80	45	0.171	0.074
80	60	0.183	0.077

Table 2.1: Poling time, electric field, leakage, and the resulting remnant polarization.

The next step in this research was to test the poled samples. Primary testing consisted of checking leakage and hysteresis of the film. These samples were still on the silicone wafer with one millimeter gold dots acting as the top electrode, and the platinum wafer surface as the bottom electrode. To connect the sample for testing, the film was removed from one edge of the wafer to expose the platinum surface. One probe from the

testing station was connected to the platinum surface, while the other was placed on top of one gold dot. This style of sample and testing resulted in a reasonable leakage current of about 10^{-8} Amps, however, the restriction of the probe on the top electrode limited the piezoelectric performance of the sample. The probe is small, but having an electrode pattern like this means that the probe connection is directly over the piezoelectrically active area. This obviously limited any mechanical movement of the material.

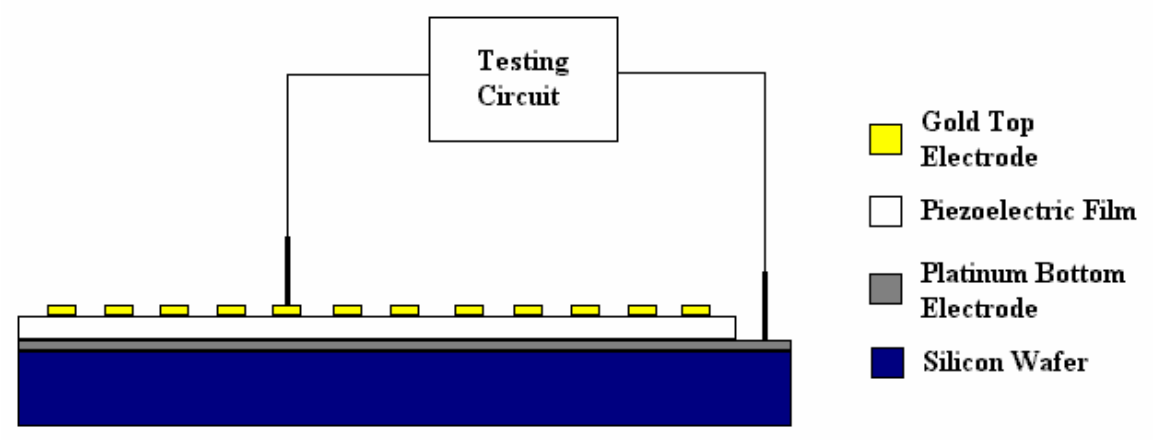

Figure 2.11: A schematic of the testing setup used with one-millimeter round electrodes.

Another problem with this style of sample and electrode was that the film material was restricted to the silicon wafer. The film must be in contact with the wafer in order to use the platinumized surface as a bottom electrode. The main objective of our research was to produce a flexible transducer, free of rigid mechanical restraint. Using the platinumized silicon wafer as a substrate and bottom electrode would not allow us to have a sample free of rigid mechanical restraint. It was obvious then that the film must be removed from the wafer, or designed so that the entire sample and both electrodes are flexible. An additional problem with this arrangement of leaving the film on the wafer

and using the platinum surface as an electrode was that the film would eventually peel away from the wafer. As the film samples aged for several days after being spun, they seemed to shrink a certain percentage until reaching a constant size. Due to the shrinking action, the films peeled away from the edges of the silicon wafer. Because of the greater surface area toward the edges of the wafer, the outer circumference of the sample had the highest amount of shrinkage, and therefore peeled away from the silicon wafer first. With a large portion of the film peeled away from the edge of the silicon wafer, very little material was left in contact with the platinum surface.

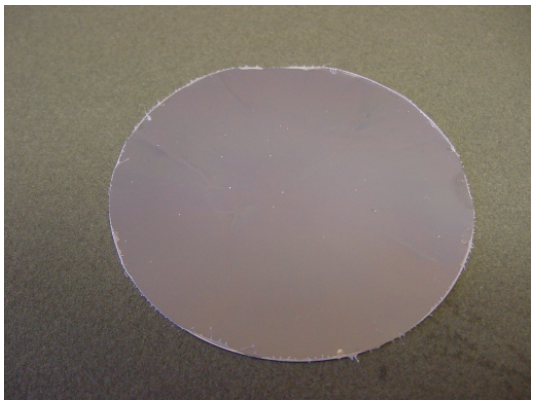

Figure 2.12: A finished copolymer film approximately 25 μm thick immediately after annealing.

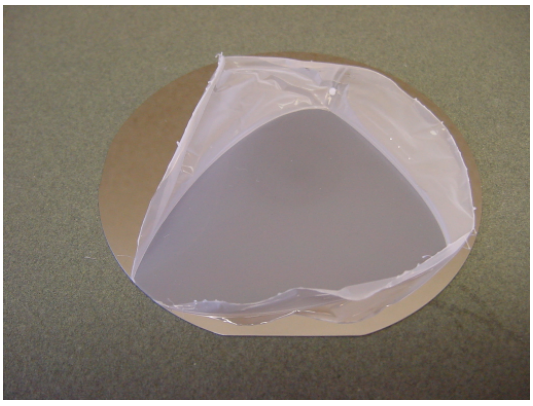

Figure 2.13: The same 25 μm thick copolymer film several days after being spun. Notice the excessive peeling around the circumference of the silicon wafer.

Figure 2.14: The figure above is of a finished composite sample approximately 20 μm thick. Each type of film sample peels away from the silicon wafer after several days of drying.

2.2.3. Characterization and Discussion of Final Film Samples

As a result of these problems, we decided to completely remove the film from the silicon wafer and then apply a gold electrode to both sides of the film by sputtering gold. To remove the films, the samples were annealed in the fume hood at about 45°C for several hours to decrease the drying time and initiate the shrinking process. Once the films were completely dry, they were carefully peeled away from the silicon wafer. In this process the silicon wafer is only used as a substrate for spin coating the film, so a platinumized surface is not necessary. The silicon wafer can also be reused after being carefully cleaned with a mild solvent. After the film was removed, the samples are masked and cut into one-inch squares. Regular bond paper was used as a mask to control

the film while being cut. The films were thin enough to stick to the paper with only the surface tension between the two surfaces. Both the sample and the paper were cut into the desired shape and size with a pair of scissors.

Next, the films were electroded by sputtering gold on both sides. This was done by using a stainless steel mask similar to the one used for the top electrode, while the sample was still on the wafer. The steel mask has a grid of one-millimeter diameter holes allowing gold to be deposited as one-millimeter dots across the surface of the sample. The cut film sample was then placed between two one-inch square masks so that gold electrodes could be sputtered on both sides of the sample. Each side was electroded one at a time with an electrode thickness of 150 nm. After electroding the samples, they were poled using the Corona Poling Station with an electric field ranging from 20 MV/m to 80 MV/m.

The poled samples were then ready to test, but this electrode pattern required that a probe on each side of the film be in direct contact with the electrodes. To do this, the film needed to be suspended so that the film was accessible on each side. This was done by placing the sample between two concentric rings with just enough clearance for the film to fit tightly. As mentioned before, PVDF has four crystal phases α, β, χ, and δ. The α phase is the most stable at room temperature, therefore, PVDF crystallizes into this phase from polymerization process. However, the β phase PVDF shows the highest piezoelectric effect of the four phases, and is formed by plastically stretching the α phase. The testing ring setup is designed to not only hold the film sample for testing, but also to stretch the film sample and keep it taut while testing.

Leakage, hysteresis, and fatigue were measured on these samples using the concentric ring setup to stretch and hold the samples while testing. Because of meager testing results, we felt that perhaps this testing setup was too restrictive on the film sample. The fact that the piezoelectric material was directly between opposing electrodes, and these electrodes were in contact with the stationary test probes, led us to think that the piezoelectric area was not able to move freely while applying an electric field. If the piezoelectric area of the sample was under constant stress from the pressure of the probe on each side, the material could not resonate and would not show any change in surface charge. To avoid this, a different electrode pattern was needed.

An electrode pattern requires that opposing electrodes be on each side of the piezoelectric area. This is what we had with the one-millimeter dot electrode pattern, but needed a different way to connect the test probes to the electrodes. Another electrode pattern was created with perpendicular lines two-millimeter wide. One line was on top of the sample, the other line was on the bottom of the sample and perpendicular to the top line. The overlapping area where the two lines intersect was then the piezoelectrically active area. The opposite ends of each electrode line were left open to connect to the testing probes. After electroding the samples, they were poled using the Corona Poling Station as explained before.

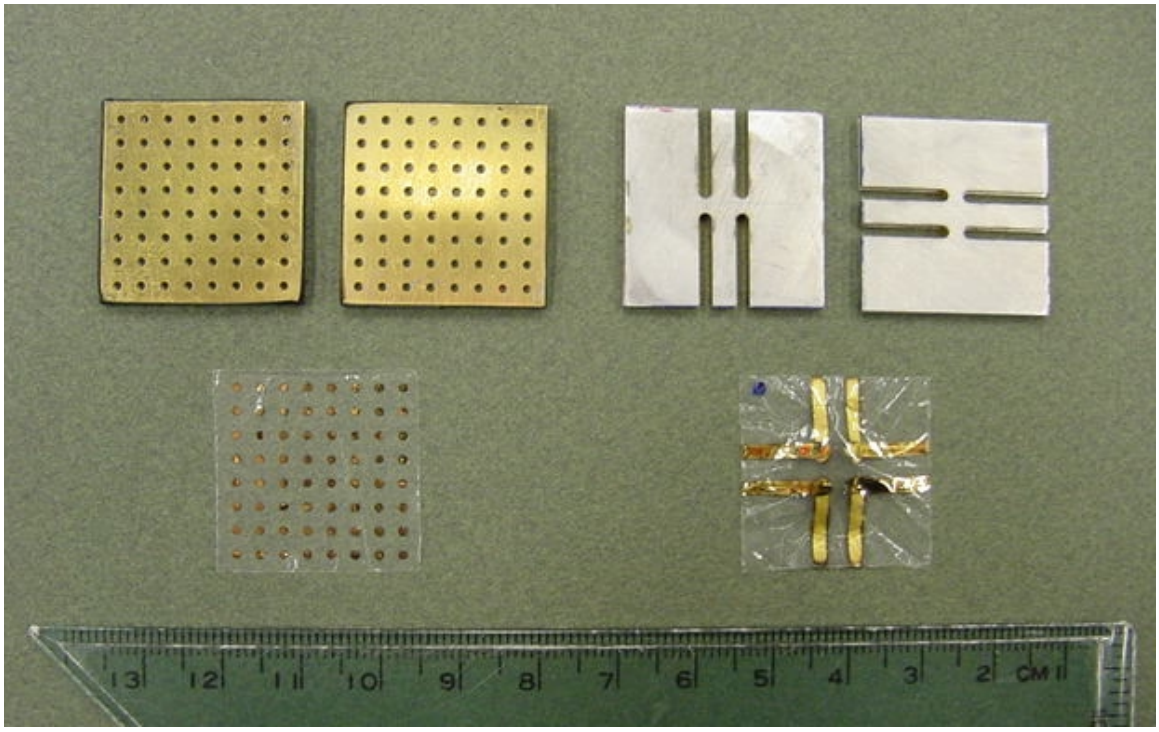

Figure 2.15: Both gold sputtering masks are shown here. The one on the left is the initial mask used, with one-millimeter dots. The mask on the right is the later mask used, with two-millimeter wide lines. The resulting electrode pattern for each mask is shown below the respective mask.

We had planned to solder a small gauge wire onto the end of each of these electrode lines that could be connected directly to the testing station. This was attempted with various sizes of wire from 75 to 250 μm and a Conductive Silver Epoxy. Due to the small size of the electrode and wire, it was very difficult to place the wire in contact with the electrode and keep it there. Curing temperature for the Silver Epoxy was also higher than the Curie Temperature of the sample material, and would destroy any polarization if employed. As a result, the epoxy was left to cure at room temperature. This resulted in a soft connection that was easily damaged. Connecting small wires to the electrode in this

manner proved to be unachievable. This led to a different connection were the gold electrodes were physically pressed against copper tabs on the concentric rings. The same electrode pattern with perpendicular lines was used for this setup, but the concentric rings were modified so that the electrode line would contact a small tab of copper on both the top and bottom of the film sample. The copper tab was then connected to a small wire, which was coupled directly to the testing machine. This arrangement worked well because the rings stretch and hold the film sample, while contacting both electrodes at the same time, and can be reused for any sample.

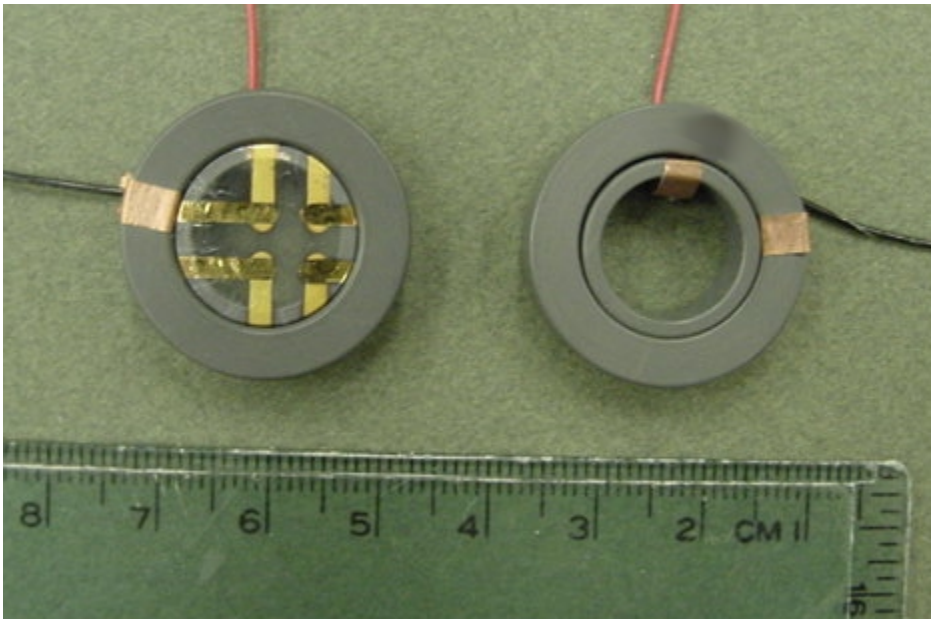

Figure 2.16: The concentric rings setup for stretching and holding the sample while making contact with the electrodes so that the testing machine can be connected to the wire leads.

CHAPTER THREE

ANALYSIS

3.1. Bulk Sample Results and Discussion

Widespread research has determined that PVDF and related polymers need an extremely high applied electric field in order to become piezoelectrically active. As discussed in Chapter 2, our inability to pole thicker bulk samples forced us to produce thinner samples. The highest voltage that we can apply with the DC power supply is about 10 kV, before the sample shorts or the power supply becomes over heated. This limits the applied electric field that we can produce for poling samples, which ultimately limits sample thickness and piezoelectric activity.

Bulk samples were originally developed in a range of 1- 3 mm thick. Due to poling restraints, sample thickness was forced to decrease to a maximum of 500 μm thick so that an adequate poling field could be applied. Samples between 500 μm and 200 μm were developed, but no further processing has taken place. Thinner samples approximately 100 μm thick were poled in an electric field of 100 kV/mm and tested for piezoelectric constant d_{33}, impedance, and hysteresis.

Although samples of this thickness could be poled well enough to test d_{33} and impedance, hysteresis is measured by applying an electric field and measuring the remnant polarization. The testing machine used for measuring hysteresis is only capable of applying 100 V through a probe station, or up to 4000 V through a high voltage amplifier and connection. The high voltage setup was used, but would not produce reliable or accurate results for these samples. Problems connecting to the electrodes and then determining what results were material properties, and what was actually electrical

noise, limited the accountability of any results obtained with this setup. The lower voltage probe station was the most accurate way to measure hysteresis, but is only capable of applying 100 V to the sample. This amount of voltage will not produce a realistic hysteresis loop for PVDF or related copolymers and composites thicker than about 75 μm. These restraints prevented us from gaining any quality results for hysteresis on the bulk samples. The impedance of the samples was measured on an Agilent 4294 A Precision Impedance Analyzer, but also resulted in unreliable results. The noise to signal ratio of the impedance test was too high to confirm the true properties of the materials. The piezoelectric constant, d_{33} for a 100 μm thick sample of 75% PVDF/TrFE and 25% PZT was found to be approximately 67 pC/N at 200Hz, for several repetitions on similar samples.

As discussed above, because of equipment limitations for poling and testing bulk samples, we were forced to develop thinner samples. It is possible to make 'bulk' samples in the range of 20 μm to 30 μm; and thus overcome problems with thickness in relation to poling electric field, testing electric field, and equipment testing ranges. However, using the same electroding procedure as before results in a sample with each electrode about as thick as the sample material. This limits the piezoelectric performance of the sample because the modulus of elasticity of the copper foil electrode is a great deal higher than that of the polymer sample, consequently limiting any mechanical performance. The solution then was to develop a thinner sample that could be processed and tested as a film.

3.2. Film Sample Results and Discussion

Results of the bulk sample experiments discussed in the previous section, and in Chapter 2, perceptibly led us to developing film samples. A great deal of research has been done on piezoelectric film production for pMUTs and MEMS. Similar processing ideas used for this research can be directly applied to polymer and composite film samples. Polymer and composite film samples for our research have been produced by spin coating a sol-gel onto silicon wafers. Sample thickness ranges from 5 μm to 65 μm, depending on sol-gel viscosity and spin rate. As mentioned before, the most consistent and highest quality samples are approximately 15 μm thick for the homopolymer, 25 μm thick for the copolymer, and 20 μm thick for the composite. The best electrode pattern used was with perpendicular two-millimeter wide lines on opposite sides of the film, which intersect over the given piezoelectrically active area. The optimal poling field and poling time seemed to be at 80 MV/m for between 15 and 30 minutes. These poling parameters have produced the highest peak polarization on all three types of samples, as shown in Table 2.1.

Primary testing consists of checking leakage and then testing hysteresis of the film samples. For consistency, all film samples tested with the concentric rings setup were tested for leakage at 50 V. These samples varied in thickness, but resulted in leakage currents of 10^{-8} to 10^{-10} Amps. For most film samples, leakage above 10^{-8} Amps indicates a capacitive material. Leakage below 10^{-8} Amps usually results in a poor hysteresis loop because of the low polar effect in the material. Clearly, these samples vary between 10^{-8} and 10^{-10} Amps, so they tend to be more capacitive. Electrode pattern and sample thickness have little effect on current leakage of the tested samples. A

complete table with nine of each type sample is shown in Appendix D. A summary of this table is shown below. Information is given for each group of samples with the same thickness.

	Thickness (um)	Poling Field (MV/m)	Leakage at 50 V (Amps)	Electrode Pattern (Sputtered Gold)
PVDF	13	80	10 E-9	two-millimeter lines
PVDF	15	80	10 E-9	two-millimeter lines
PVDF	26	80	10 E-9	two-millimeter lines
PVDF/TrFE	25	80	10 E-9	two-millimeter lines
PVDF/TrFE	30	80	10 E-10	two-millimeter lines
PVDF/TrFE	64	80	10 E-10	two-millimeter lines
PVDF/TrFE/PZT	13	80	10 E-9	two-millimeter lines
PVDF/TrFE/PZT	20	80	10 E-8	two-millimeter lines
PVDF/TrFE/PZT	38	80	10 E-9	two-millimeter lines

Table 3.1: Sample thickness, poling field, electrode pattern, and leakage tested on the probe station with an application of 50 volts to each sample.

After testing leakage, the samples were ready for hysteresis testing. Parameters that can be varied while testing hysteresis are maximum applied voltage, loop period, delay before measurement, bias, and whether or not the electric field is switched (monopolar or bipolar). The maximum applied voltage is simply the maximum voltage reached at the inflection point on the first leg of the hysteresis loop. The period of the loop is a measure of how long the sample is tested, and how many measurements are taken; this translates into the number of points seen on the hysteresis plot. Delay before the test loop measurement is the amount of time waited after the preset loop. A preset loop is applied to the sample to ensure that the dipoles of the sample are oriented in a known direction before measuring polarization. A delay between the preset loop and the

test loop is commonly used to allow parasitic effects to settle to an inactive state. Bias is a function that will add a preset voltage to each point on the hysteresis loop, thus offsetting the loop on the y-axis.[20] The applied electric field for a standard hysteresis is switched from positive to negative to measure the ability of the polar dipoles to switch direction. Switching polarity is not necessary to measure remnant polarization, and is not required for our research. Our samples are pre-poled, so applying a bipolar field would destroy any polarization in the sample when the electric field is switched. This is avoided by using a monopolar electric field. A monopolar electric field can be applied in either the positive or negative direction, depending on the orientation of the dipoles resulting from poling. A monopolar electric field does not change polarity during the hysteresis test, resulting in a one-sided hysteresis loop.

The probe station was used to measure hysteresis and peak polarization on all three types of samples. This means that 100 volts is the maximum available voltage to drive the sample. On samples 25 μm thick, this results in an electric field of 4 kV/mm. This is only about one-quarter of the electric field that is needed to see any significant piezoelectric response. Despite only being able to apply a relatively minimal electric field, several tests were done to measure peak and remnant polarization at different voltages. Many voltages were experimented with, but for simplicity, four voltages were recorded for each sample. Voltages of 25, 50, 75, and 100 were applied to nine samples of each type, with the peak polarization recorded for each. A drive voltage of 100 volts produced the highest peak and remnant polarization for each sample. The average peak polarization for 15 μm thick PVDF samples is about 0.042 $\mu C/cm^2$ with an applied electric field of 6.67 kV/mm. For the 25 μm thick copolymer samples, the average peak

polarization is about 0.054 μC/cm^2 with an applied electric field of 4.0 kV/mm. The 20 μm thick composite samples naturally produced the highest peak polarization of about 0.075 μC/cm^2 with an applied electric field of 5.0 kV/mm.

A complete table of peak polarization for each of nine films tested for each type of sample is shown in Appendix E. A summary of this table with average peak polarization at 100 volts for each thickness of sample is shown below.

	Thickness (um)	Poling Field (MV/m)	Applied Field (MV/m) at 100 V	Peak P (uC/cm^2) of 100 V hysteresis
PVDF	13	62	7.692	0.04167
PVDF	15	80	6.667	0.04167
PVDF	26	80	3.846	0.03867
PVDF/TrFE	25	32	4.000	0.03933
PVDF/TrFE	30	80	3.333	0.05367
PVDF/TrFE	64	80	1.563	0.04767
PVDF/TrFE/PZT	13	62	7.692	0.04500
PVDF/TrFE/PZT	20	80	5.000	0.07467
PVDF/TrFE/PZT	38	80	2.632	0.06833

Table 3.2: A table of average values for nine films of each type material showing the thickness, poling electric field, applied field for testing, and the corresponding peak polarization.

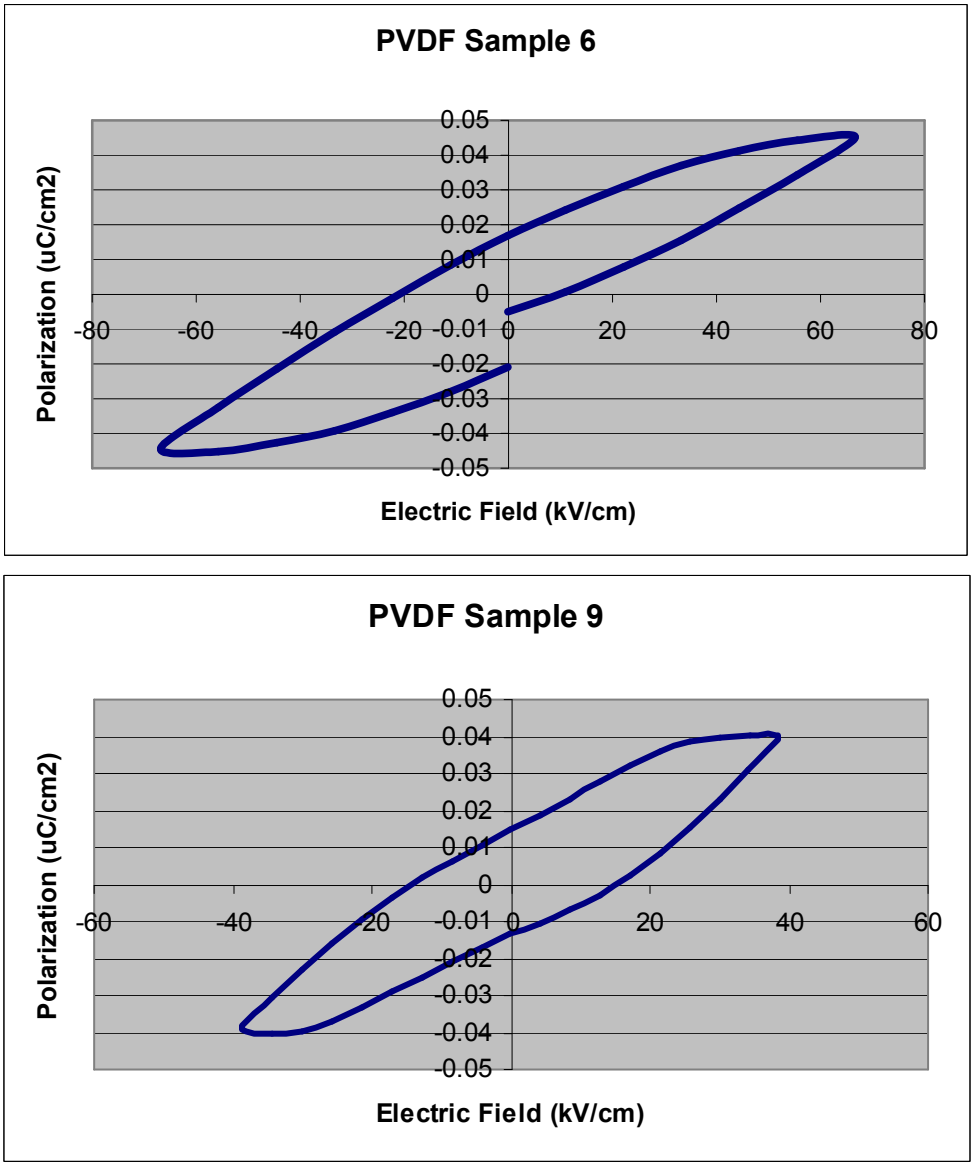

Figure 3.1: Electric field versus polarization hysteresis plots for homopolymer samples 6 and 9. Sample 6 is the thinner of the two, and therefore has a higher applied electric field, resulting in a higher peak polarization.

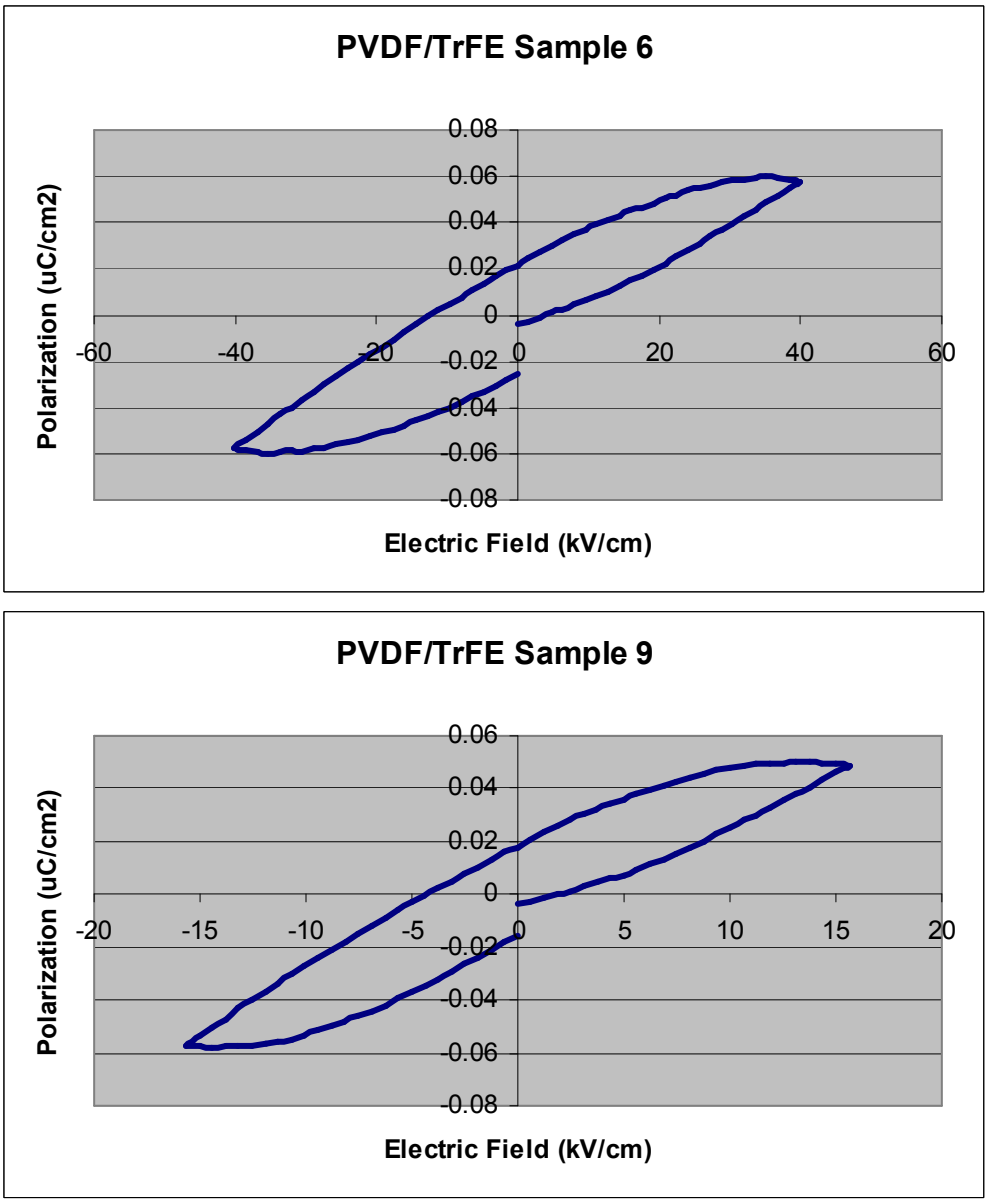

Figure 3.2: Hysteresis plots for copolymer samples 6 and 9. Again, sample 6 is the thinner of the two, resulting in a higher applied electric field and higher peak polarization.

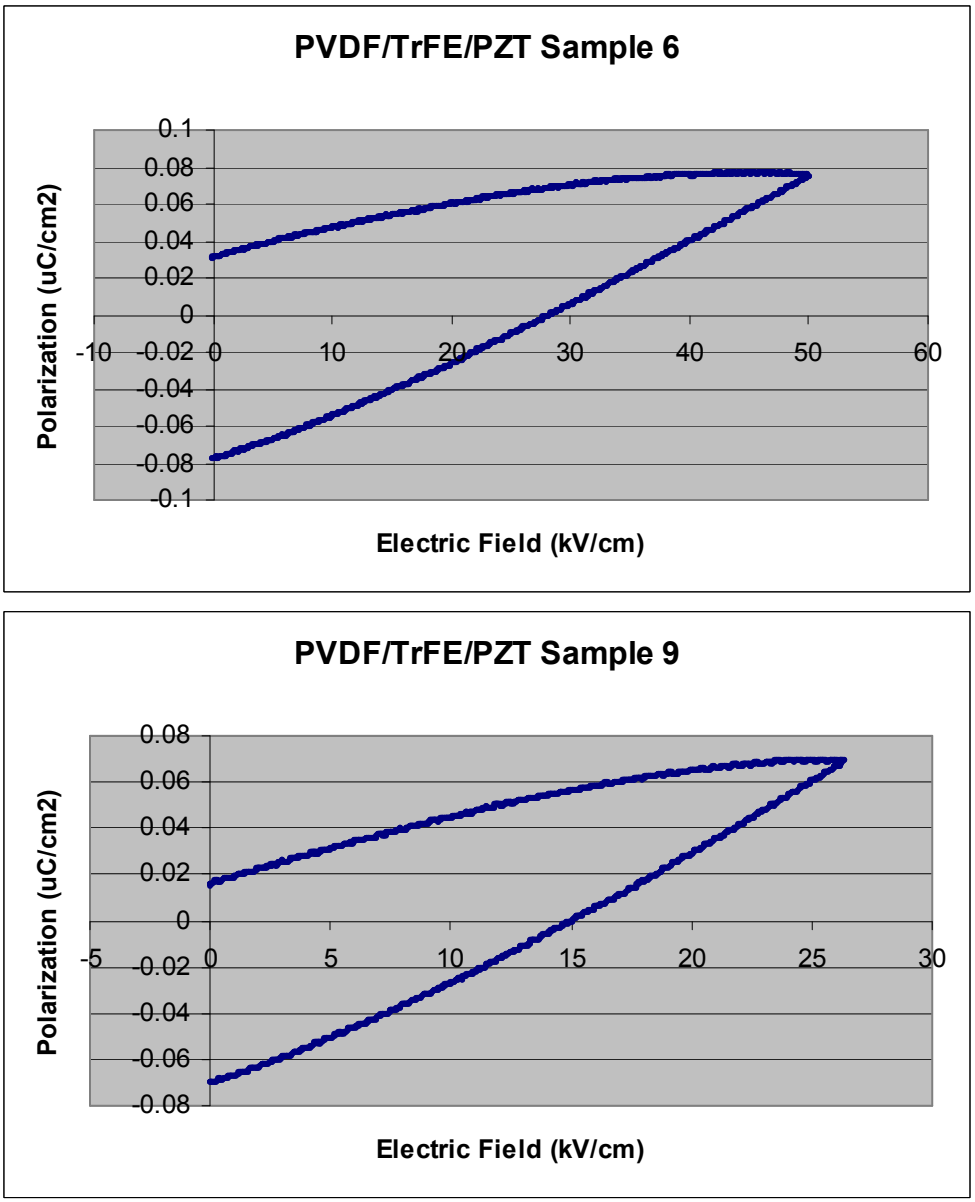

Figure 3.3: Two monopolar hysteresis plots for composite samples 6 and 9. Sample 6 is the thinner than sample 9, so the applied electric field and peak polarization are higher.

As can be seen in Table 3.2, peak polarization for each of the same type of samples varies quite a lot, but there is definitely a difference in peak polarization between types of samples. Concurring with the vast amount of research on PVDF/TrFE, the copolymer material produces an average higher peak polarization at a lower applied electric field than the homopolymer. Also as expected, the average peak polarization of the composite material is highest of the three sample types. The 13 μm thick samples were the thinnest samples of the composite material, and therefore had the highest applied electric field used for testing. For some reason though, they also have the lowest peak polarization of the composite samples. This may be due to some kind of dielectric breakdown on such a thin film. Although PVDF and related piezoelectric materials generally need a very high-applied electric field, these films may be thin enough to breakdown under such a high electric field. The high electric field may cause some intrinsic breakdown, which increases dielectric loss, resulting in more heat generation. The added heat generation could then likely cause some thermal breakdown.

To compare these results with others, both the material and electric field must be considered. Eiichi Fukada reported a peak polarization of 9.5 $\mu C/cm^2$ for a PVDF film sample with an applied electric field of 240 kV/mm. Similar results from Pierre Ueberschlag report a peak polarization of 9.5 $\mu C/cm^2$ for a 25 μm thick PVDF film with an applied electric field of 300 kV/mm. Eberle, Schmidt, and Eisenmenger reported a peak polarization of 5 $\mu C/cm^2$ with an applied electric field of 120 kV/mm for a 50/50 copolymer film sample. They also reported another copolymer film sample with a peak polarization of 7.4 $\mu C/cm^2$ with an applied electric field of 160 kV/mm, and a third with a peak polarization of 3.5 $\mu C/cm^2$ with an applied electric field of 80 kV/mm. Very few

research results have been published for polymer/ceramic piezoelectric composites like the ones developed in this research. However, our results with composite material can be compared to our results, and published results of PVDF and PVDF/TrFE.

One batch of samples was sent to J&W Medical LLC, in Connecticut, for similar characterization as done in our lab, although they were able to apply a much higher electric field. They tested a 15 μm thick sample of homopolymer, a 25 μm thick sample of copolymer, and a 20 μm thick sample of composite material. The samples were pre-poled in an electric field of 53, 32, and 40 kV/mm for the homopolymer, copolymer, and composite sample, respectively. With an applied electric field of 15 kV/mm, the homopolymer sample was destroyed and did not produce any results. The copolymer sample had an applied electric field of 15.78 kV/mm, to produce a peak polarization of 0.25 $\mu C/cm^2$. The composite sample was tested with an applied electric field of 15.5 kV/mm to produce a peak polarization of 1.81 $\mu C/cm^2$. Although the results are lower than some published values for PVDF and PVDF/TrFE, the homopolymer and copolymer samples produced a peak polarization proportionally comparable to other published values, considering the difference in applied electric field. The composite material has a noticeably higher peak polarization than either the homopolymer or copolymer, so the addition of PZT obviously increases the piezoelectric response.

	Thickness	Poling Field	Leakage at 50 V	Electrode Design	Applied Voltage	Applied Field	Peak P
	(um)	(MV/m)	(Amps)	(Sputtered Gold)	(Volts)	(MV/m)	(uC/cm2)
PVDF	15	53	10 E-9	one-millimeter dots	225	15.00	no results
PVDF/TrFE	25	32	10 E-9	one-millimeter dots	375	15.78	0.25
PVDF/TrFE/PZT	20	40	10 E-10	one-millimeter dots	300	15.5	1.81

Table 3.3: Samples tested with high voltage setup. Applied voltage was significantly higher than previous tests, resulting in a higher applied electric field and higher resulting peak polarization.

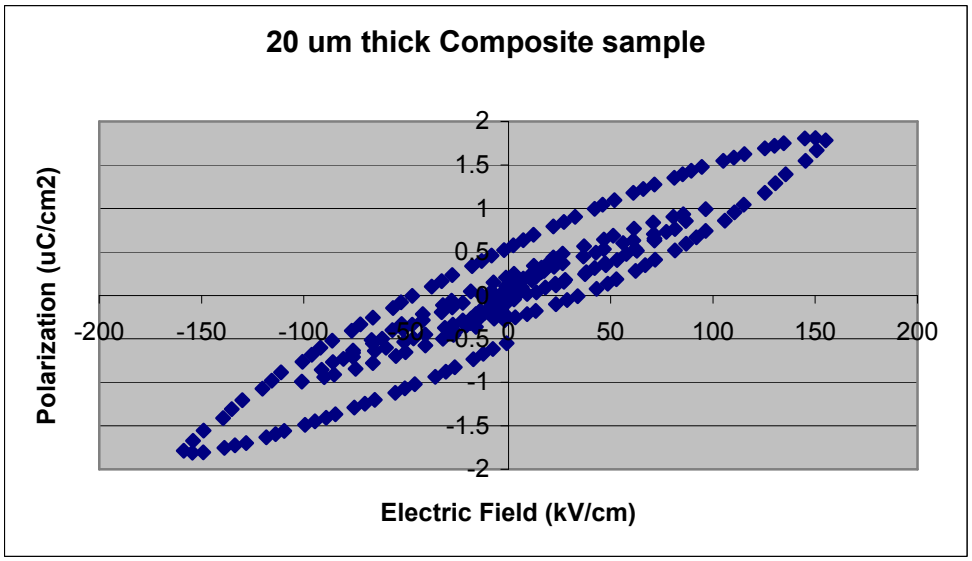

Figure 3.4: Electric field versus polarization hysteresis loop for the 20 μm thick composite sample tested with the high voltage setup.

Capacitance, dielectric loss tangent (tan δ), dielectric constant K, and piezoelectric constant d_{33} were also tested. Each sample had 64 one-millimeter round electrodes. Of these, 25% were randomly tested. The average capacitance for the homopolymer sample is 8.35 pF. The average capacitance for the copolymer sample is 2.98 pF, while the average capacitance for the composite sample is 50.32 pF. Clearly, the

addition of PZT to the copolymer produces a large increase in capacitance, and thus increases its charge storing capacity. The average dielectric loss tangents for the homopolymer, copolymer, and composite are 0.03585, 0.05805, and 0.0563, respectively. So the addition of PZT to the copolymer does not seem to increase the dielectric loss tangent. The dielectric loss tangent for these homopolymer and copolymer samples is slightly higher than reported values of commercial material. Reported dielectric loss tangent values for PVDF and PVDF/TrFE are 0.0289 and 0.0229. The average K values are; 18.038 for the homopolymer, 10.741 for the copolymer, and 144.86 for the composite. The dielectric constant K was measured at 1 kHz for each of the samples. The copolymer has an average K, at 1 kHz, slightly above the reported values for thicker samples of this material. However, the average K value for the homopolymer sample is much higher than the reported values. This could be due to the application of a fairly high electric field to such a thin sample during poling, resulting in better alignment of polymer chains. Predictably, the composite has a significantly higher K value than the other two samples. The addition of 25% PZT by volume to the 50/50 PVDF-TrFE copolymer increased the K value by approximately 14 times. The tables below shows the results discussed above, as well as a comparison to commercial PVDF and PVDF/TrFE.

	Thickness	Electrode Diameter	Capacitance	Dielectric loss tangent	Dielectric constant	
	μm	mm	pF	tan δ	K	
Homopolymer	15	1	8.35424	0.03585	18.03787	**AVG**
			0.45271	0.00812	0.97745	**STDV**
Copolymer	25	1	2.98490	0.05805	10.74130	**AVG**
			0.44504	0.00768	1.60150	**STDV**
Composite	20	1	50.31731	0.05629	144.85534	**AVG**
			6.03293	0.01346	17.36783	**STDV**

Table 3.4: Dielectric test results.

	Our Samples		Commercial Values	
	PVDF	**PVDF-TrFE**	**PVDF**	**PVDF-TrFE**
K	18.04	10.74	11.89	7.45
tan δ	0.03585	0.05805	0.02890	0.02290
d33 (pC/N)	30-37	30-37	32-35	32-35

Table 3.5: Dielectric and piezoelectric properties of the PVDF and PVDF/TrFE of our samples compared to those of commercial PVDF and PVDF/TrFE.

Three samples were also tested for piezoelectric constant d_{33}. Each sample has 64 one-millimeter round electrodes, so d_{33} measurement was attempted on individual electroded areas using two sharp probes. No data was obtained this way, most likely because the connection between the probes and electrodes was inadequate. We found that the sharp electrodes on the probe station would actually puncture the electroded area if applied directly on top of the piezoelectrically active area. As a result, the probes do not make a good connection with the electroded surface. Instead of measuring the individual d_{33} value for each electroded area, several electroded areas were tested simultaneously with two flat probes. The average d_{33} value of the homopolymer and copolymer samples was in the range of 30-37 pC/N. These values are very close to other

published values for PVDF and PVDF/TrFE as shown in Table 3.5 above. The composite sample had a d_{33} value of about 37 pC/N. This seems somewhat low for this type of composite poled in such a high electric field, but it is still at least if not slightly greater than the d_{33} value for the homopolymer and copolymer.

The lower value of piezoelectric coefficient d_{33} for the composite material may be explained as a result of the type of composite that it is. In these 0-3 ceramic/polymer composites, the ceramic is distributed as a powder within the polymer matrix. With the highly piezoelectric PZT powder dispersed in the polymer, dielectric properties in the composite will show improvements because they are based on the materials charge storing properties in a DC voltage. However, the piezoelectric coefficient d_{33} does not show a large improvement because it is a measure of the resulting surface charge per unit force. Most of the force applied to these composites produces a piezoelectric response in only the polymer. Because the polymer is the surrounding substance of the ceramic powder, and because the polymer is significantly more elastic than the ceramic powder, there is very little mechanical influence on the ceramic powder. The stress created in the composite materials as a result of an applied force is almost completely absorbed by the polymer material, without creating enough stress on the ceramic powder to induce polarization. As a result, these materials will have an improved dielectric constant, but low piezoelectric constant.

All three types of samples were also tested for fatigue on our probe station. Leakage, hysteresis, and fatigue were all measured using the concentric rings setup to stretch and hold the samples while testing. Fatigue is measured by using a pulse polarization test. The pulse polarization test consists of five symmetric pulses separated

by one-second intervals. The first pulse is in the negative directions (-Vmax). This presets the dielectric material and serves the same function as the preset loop for the hysteresis test. The second pulse is to the maximum positive voltage (+Vmax). A single measurement is taken at the top of the second pulse to record the total polarization transferred from the dielectric material as the voltage increases from the first pulse. Because the direction of polarity was switched between the first and second pulse, the second pulse actually measures switching polarization of the material. After the polarization measurement is taken on top of the third pulse, the voltage decreases to zero for a second measurement. This measurement records the value of any polarization left in the sample at the end of the loop. The third pulse is initiated one second later, to +Vmax again. Two measurements are again taken here. One at the top to measure total polarization, and one at the bottom of the pulse to measure remaining polarization. Because the sample was already charged in the positive direction before this pulse, the direction of polarity is not switched. As a result, the third pulse measures unswitched charge. The difference between the top and bottom measurements of the third pulse, and the top and bottom measurements of the second pulse is the remnant polarization. The fourth and fifth pulses are exactly opposite of the second and third pulses, going to – Vmax twice in a row.[20]

A single pulse consists of five parts. The first is the delay period before the pulse is applied. The second is the amount of constant voltage applied during the delay period. The next part is the ramp to the pulse voltage, followed by the delay at the pulse voltage for an assigned amount of time, depending on pulse width. The pulse width includes the ramp time. The last part is the ramp to the end voltage and another delay for the assigned

pulse width. Each of these five parts can be tailored in many ways to create a custom pulse. The five parameters needed for each pulse are: the delay period, delay voltage, pulse width, pulse voltage, and end voltage. Each pulse can be custom designed, or the same pulse can be used repeatedly.

The standard pulse polarization test used in our lab is the PUND. This is an acronym for Positive Up, and Negative Down. For the PUND, pulse width, pulse voltage and delay time can be changed. The delay and end voltage is fixed at zero. The standard test also has a delay time of 1.0 second, but can be changed if desired. Samples 5-9 of each type of sample were fatigue tested with a standard pulse polarization test repeated 50 times at 500 Hz.

Samples 5-9 of each type of sample were fatigue tested with an applied voltage of 100. The corresponding electric field for each sample is the same as shown above in Table 3.2 at 100 volts for samples 5-9. The pulse width for all three types of samples is 0.01 ms, the pulse voltage is 100 volts, and the delay time is 1.0 ms. The peak polarization for the homopolymer sample is approximately 0.036 $\mu C/cm^2$. Although the peak polarization varies from 0.01 $\mu C/cm^2$ to 0.036 $\mu C/cm^2$, the sample seems to retain its piezoelectric response for at least 10^5 cycles. The copolymer sample has a peak polarization that varies from about 0.01 to 0.038 $\mu C/cm^2$ for 10^5 cycles. The peak polarization of the composite sample varies between 0.03 and 0.064 $\mu C/cm^2$ for 10^5 cycles.

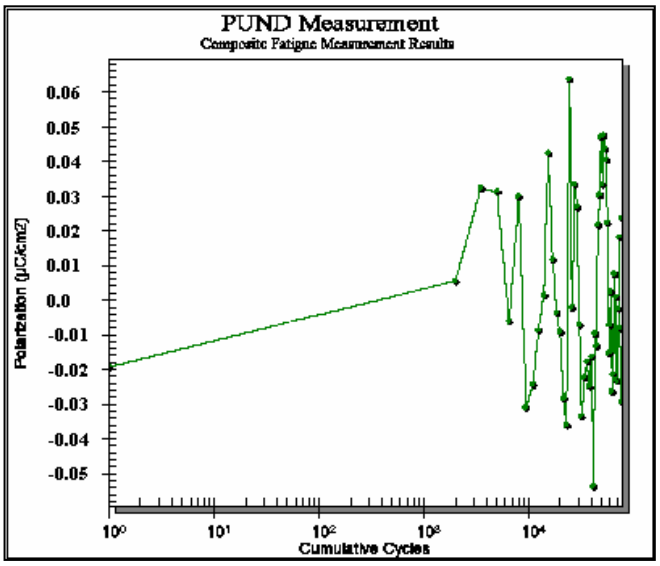

Figure 3.5: This plot is of a 20 μm thick composite fatigue test. Applied voltage is 100 volts, pulse width is 0.01 ms, and delay time is 1.0 ms.

Fatigue test plots for all three types of material looked similar to Figure 3.6. No obvious trends can be seen in these plots, but they at least show that there is no extreme ferroelectric fatigue under the conditions outlined above. Fatigue testing under different parameters is needed to learn more about ferroelectric fatigue of the composite material. These fatigue results provide only a beginning point for further research. Testing the samples with a higher number of cycles and at a higher frequency would likely provide more meaningful data.

As discussed in Section 1.2.1, PVDF and copolymers retain a high percentage of their remnant polarization for many years. The polar behavior of PVDF has been found to be very robust at room temperature, even after many years and at high numbers of cycles. The polar behavior of PZT is obviously also quite stable at room temperature,

under mild conditions, such as these samples were tested. This composite material would most likely be applied in a fixed condition where temperature is controlled. In harsh conditions, high temperature and extremely high electric field, the material may develop dielectric breakdown. Dielectric breakdown results from several factors including sample thickness, operating temperature, electrode composition and shape, and the porosity of the material. Under extreme conditions, PVDF may display either intrinsic or thermal breakdown.[21] The intrinsic effect will result if too high of an electric field is applied. Thermal breakdown will happen to PVDF, and related materials, if they are used in an ambient temperature close to the Curie Temperature.

PVDF and related materials are also subject to depolarization, as with any other dielectric material. PVDF is very electro-negatively stable, so it resists depolarization unless extreme mechanical or thermal stresses occur. Mechanical depolarization happens when the mechanical stress on the dielectric material becomes high enough to disturb the orientation of the domains, and thus destroy the alignment of the dipoles. Thermal depolarization is simply when the domains become disoriented because the material is heated above its Curie Temperature.[21] The dipoles of the material become completely disorganized, resulting in depolarization.

Obviously, the film samples have allowed us to study the piezoelectric properties of PVDF and related materials, within the ranges of our own lab equipment. The bulk samples likely have similar properties as the film samples, and can be applied to many of the same applications. Although the film samples do not have extraordinary properties as compared to piezoelectric ceramics, the film samples have served their purpose well in our research.

3.3. Conclusion and Recommendations

The main objective of this research was to further improve the piezoelectric properties of PVDF and its copolymer with TrFE, while maintaining the original flexibility of the polymers. The primary method of reaching this objective was by developing a 0-3 composite material with a piezoelectric ceramic, such as lead zirconate titanate (PZT). As can be seen in the results, the addition of PZT to the copolymer does increase the piezoelectric response. Another goal of this research was to develop the processing of these materials so that they can be easily made, and with repeatable results. The results shown in Table 3.2 prove that the composite material does have improved piezoelectric properties over the homopolymer and copolymer. It is also apparent from Table 3.2 that the results are repeatable. The processing of these materials has greatly evolved, and could be easily adapted to higher quantities or different sizes of samples. The piezoelectric properties of these composites can be improved on, but the processing science developed in this research is solid, and can be used to guide future studies. The discussions in sections 2.1 and 2.2 review the complete fabrication process for both the bulk samples and the film samples.

Another goal of this research was to apply the developed materials to certain devices, such as flexible transducers and ultrasonic equipment. However, more time was spent on developing and processing a composite material with quality and repeatable results than was expected. This composite material has not been applied to any particular devices yet, but we have made a large advancement in the processing of such a material. We have also realized, for certain reasons explained in section 3.2, that the dielectric

properties of the composite material are improved, but the electromechanical properties remain very similar to the base polymers. This fact limits the materials use as a transducer, but may promote its use as a flexible dielectric material. With the progress made in processing piezoelectric ceramic/polymer composites, applications to certain piezoelectric devices is inevitable.

In conclusion, this research project has:

A) developed the processing science necessary to incorporate ceramic powders uniformly into the base polymers, without losing the flexibility of the base polymers.

B) characterized the composites in order to understand the influence of the piezoelectric ceramic powders on the electromechanical properties of the composites

C) fabricated simple and reproducible materials capable of being applied to various devices

One suggestion for future work would be to process and test different compositions of PVDF/TrFE/PZT. Compositions of 15/85 and 35/65 PZT to PVDF/TrFE were made, but no further processing was done. It is assumed that the exact same processes could be used to develop and test samples of different compositions. Compositions with a higher concentration of PZT would likely have a better piezoelectric response. A composite with up to 35% PZT by volume should retain most of the flexibility of the base polymer.

Another suggestion for future work would be to develop a different electroding pattern that would allow testing with flat probes. Gold electrodes about one-centimeter in diameter would allow a solid connection to the sample using the high voltage setup. This

would allow testing of leakage, hysteresis, and fatigue with an applied voltage up to 4000 volts. There have been problems with the high voltage setup and test results, but these problems could no doubt be solved. One key to producing better piezoelectric results for these polymer and composite materials is being able to supply a high enough electric field for testing.

SUMMARY

Significant research has been conducted on PVDF and copolymers as a result of the piezoelectric effects found in these materials. Although piezoelectricity does exist in these semi-crystalline polymer materials, the piezoelectric response of PVDF is quite small compared to that of most piezoelectric ceramics. It is evident though, that copolymers such as trifluoroethylene (TrFE) and tetrafluoroethylene (TFE) help to improve the piezoelectric response in PVDF by improving the crystallinity. Further improvements were made by developing a 0-3 composite material with PZT and PVDF.

As expected, piezoelectric ceramic materials are excellent candidates for use in solid-state applications like transducers and micro-electrical-mechanical devices. However, two limiting factors of piezoelectric ceramics are the high stiffness and the relatively higher cost of fabrication. These are the primary reasons that piezoelectric polymers have been studied so extensively. Piezoelectric polymers are very flexible, easy to fabricate, and have an acoustic impedance comparable to soft human tissue. Ultimately, a material with the mechanical properties of a polymer like PVDF, and the piezoelectric properties of a ceramic like PZT, would be ideal for many piezoelectric applications. The goals of this research project are based on these ideas, and the applications of such a material.

The main objective of this research was to further improve the piezoelectric properties of PVDF and its copolymer with TrFE by developing a 0-3 composite material with PZT, while maintaining the original flexibility of the polymers. As can be seen in Chapter 3, the addition of PZT to the copolymer does increase the piezoelectric response. Another goal of this research was to develop the processing of these materials so that

they can be easily, and repeatedly, made with consistent results. This has been done, and is discussed in further detail in Chapters 2 and 3.

Bulk samples were originally developed in a range of 1- 3 mm thick, but as discussed in Chapter 2, our inability to pole thicker bulk samples forced us to produce thinner samples (less than 0.5mm). Applied voltage limitations have consequently limited sample thickness. Samples between 500 μm and 100 μm were developed, with testing only on the 100 μm thick samples. These 100 μm thick samples were poled in an electric field of 100 kV/mm and tested for piezoelectric constant d_{33}, impedance, and hysteresis. Because of difficulties with testing, repeatable results were found only for piezoelectric constant d_{33}. The piezoelectric constant, d_{33} for a 100 μm thick sample of 75% PVDF/TrFE and 25% PZT was found to be approximately 67 pC/N at 200Hz. Limitations on applied voltage have obviously limited our ability to process and characterize these samples. The most straightforward solution to these processing and characterization problems was to develop a thinner sample that could be processed and tested as a film.

Similar processing ideas used for piezoelectric film preparation and MEMS research were directly applied to polymer and composite film samples. Polymer and composite film samples were produced for this research by spin coating a sol-gel onto silicon wafers. As mentioned in Chapter 3, the most consistent and highest quality samples are approximately 15 μm thick for the homopolymer, 25 μm thick for the copolymer, and 20 μm thick for the composite.

Two electrode patterns are used, depending on the testing setup available. The first electrode pattern was with one-millimeter dots placed in a grid approximately five-

millimeters apart, with an identical pattern on the opposite side of the film. The second, and final electrode pattern on the film samples was with perpendicular two-millimeter lines on opposite sides of the film, which intersect over the given piezoelectrically active area. As discussed in section 2.2.2, the optimal poling field and poling time was at about 80 MV/m for between 15 and 30 minutes.

The first measurement taken for each sample is the electrical leakage, which is measured on the probe station. Leakage on the film samples with an applied voltage of 50 volts was in the range of 10^{-8} to 10^{-10} Amps, indicating that the samples tend to be more capacitive. Hysteresis was also tested on the probe station with applied voltages of 25, 50, 75, and 100 volts. A complete table of the corresponding peak polarization for each sample at these applied voltages is given in Chapter 3 (Table 3.2). Even though we were only able to apply a relatively minimal electric field, several tests were done to measure peak and remnant polarization at the above voltages. Perceptibly a drive voltage of 100 volts produced the highest peak and remnant polarization for each sample. The average peak polarization for 15 μm thick PVDF samples is about 0.042 $\mu C/cm^2$ with an applied electric field of 6.67 kV/mm. For the 25 μm thick copolymer samples, the average peak polarization is about 0.054 $\mu C/cm^2$ with an applied electric field of 4.0 kV/mm. The 20 μm thick composite samples naturally produced the highest peak polarization of about 0.075 $\mu C/cm^2$ with an applied electric field of 5.0 kV/mm.

Although these values are small, they are proportionately comparable to other reported values for PVDF and PVDF/TrFE, when comparing the applied electric field and resulting peak polarization. Only a small number of research results have been published for polymer/ceramic piezoelectric composites, particularly 0-3

PZT/PVDF/TrFE composites like these. However, our results with composite materials can be compared to published results, and our own results for PVDF and PVDF/TrFE. As can be seen in Table 3.2, there is definitely a difference in peak polarization between types of samples, with the highest values belonging to the composite material.

One batch of samples was sent to J&W Medical LLC for characterization, where a higher electric field could be applied to the samples. With an applied electric field of 15 kV/mm, the 15 μm thick homopolymer sample was destroyed and did not produce any results. The 25 μm thick copolymer sample had an applied electric field of 15.78 kV/mm, to produce a peak polarization of 0.25 $\mu C/cm^2$. The 20 μm thick composite sample was tested with an applied electric field of 15.5 kV/mm to produce a peak polarization of 1.81 $\mu C/cm^2$. Once again, the results are lower than some published values for PVDF and PVDF/TrFE, but the homopolymer and copolymer samples produced a peak polarization proportionally comparable to other published values reported for these materials. As expected, the composite material had a noticeably higher peak polarization than either the homopolymer or copolymer.

Further characterization of each type of sample included testing of capacitance, dielectric loss tangent (tan δ), dielectric constant K, piezoelectric constant d_{33}, and fatigue. These results continued to show comparable results for PVDF and PVDF/TrFE as reported from various sources, and noticeably improved piezoelectric properties for the composite material. The composite has a significantly higher K value than the other two samples, increasing the dielectric constant by approximately 14 times. The results of the fatigue tests confirmed that PVDF and PVDF/TrFE retain a high percentage of their remnant polarization for many cycles, under mild conditions.

In general, we have successfully reached the goals of this research project; most significantly, a 0-3 piezoelectric composite has been developed and refined. Major advances achieved in this research are the development of the processing science necessary to create such a composite, and characterization of these composites. The resulting processes are capable of producing simple and reproducible samples, that can potentially be applied to several piezoelectric devices. Although the piezoelectric properties of these composites are not extraordinarily good, the processing science developed in this research is fundamental, and can be used for further work. More advances in improving the piezoelectric effects of these composite materials will likely follow with the processing science and resulting characterization developed in this research.

REFERENCES

1. Cady, W.G. Piezoelectricity. New York: McGraw-Hill Companies, 1946.
2. Seymour, R.B., and G.B. Kauffman. "Piezoelectric Polymers." Products of Chemistry 67.9 (1990) 763-765.
3. Barsoum, M. Fundamentals of Ceramics. New York: McGraw-Hill Companies, 1997.
4. Kasap, S.O. Principles of Electronic Materials and Devices. 2nd ed. New York: Mcgraw-Hill Companies, 2002.
5. Haertling, G.H. "Ferroelectric Ceramics: History and Technology." Journal of the American Ceramic Society 82.4 (1999) 797-818.
6. Safari, A., R.K. Panda and V.F. Janas. "Ferroelectricity: Materials, Characteristics and Applications." Key Engineering Materials 122-124 (1996) 35-70.
7. Sessler, G.M., and A. Berraissoul. "LIPP Investigation of Piezoelectricity Distributions in PVDF Poled with Various Methods." Ferroelectrics 76 (1987) 489-496.
8. Sessler, G.M. "Charge Storage in Dielectrics." IEEE Transactions on Electrical Insulation 24.3 (1989) 395-402.
9. Peterson, K. E. "Silicon as a Mechanical Material." Proceedings of the IEEE 70.5 (1998): 420.
10. Schwartz, R.W., J. Ballato, and G.H. Haertling. "Piezoelectric and Electrooptic Ceramics." University of Missouri-Rolla (2003) <www.umr.edu/index.phpresearch>.

11. Eberle, G., H. Schmidt, and W. Eisenmenger. “Piezoelectric Polymer Electrets.” IEEE Transactions on Dielectrics and Electrical Insulation 3.5 (1996) 624-646.

12. Tamura, M. “Piezoelectric Polymer Properties and Potential Applications.” Ultrasonic Symposium Proceedings (1987) 344-346.

13. Palta, S.P., L.M. Blinov, and V.M. Fridkin. “Physics of Two-Dimensional Ferroelectric Polymers.” Institute of Crystallography, Russian Academy of Sciences (2003) <www.ns.crys.ras.ru>.

14. Fukada, E. “New Piezoelectric Polymers.” Japanese Journal of Applied Physics 37 (1998) 2775-2780.

15. Broadhurst, M. “Polymer Physics.” Physics Today January (1994) 51-52.

16. Fukada, E. “History and Recent Progress in Piezoelectric Polymer Research.” 1998 IEEE Ultrasonics Symposium (1998): 597-605.

17. Harrison, J.S. and R.J. Silcox. “Piezoelectric Materials for Sensor and Actuator Applications at NASA Langley Research Center.” Sensor and Actuators 8.2 (1999) 15-27.

18. Marra, S.P., K.T. Ramesh, and A.S. Douglas. “Mechanical Properties of Compliant Piezoelectric Composites.” Department of Mechanical Engineering, The Johns Hopkins University (2000) <www.me.jhu.edu>.

19. Bandyopadhyay, A., and S. Bose. “Processing and Characterization of 0-3 Composites for Flexible Transducers.” School of Mechanical and Materials Engineering Research Proposal, Washington State University (2001).

20. Radiant Technologies, Inc. Precision Materials Analyzer Vision Program for Workstation Ferroelectric Test System. Albuquerque, NM: Radiant Technologies, Inc., 2000.
21. Gerhard-Multhaupt, R. "Polyvinylidene Fluoride: A Piezo-, Pyro-, and Ferroelectric Polymer and its Poling Behavior." Ferroelectrics 75 (1987) 385-396.
22. Ueberschlag, P. "PVDF Piezoelectric Polymer." Sensor Review 21.2 (2001) 118-125.
23. "Piezoelectric Ceramics: Properties and Applications." Morgan Electro Ceramics (2003) <www.morganelectroceramics.com>.
24. "Properties of TRS' Standard Piezoceramics." TRS Ceramics (2003) <www.trsceramics.com>.
25. Mark, J.E. Polymer Data Handbook. New York: Oxford University Press, 1999.
26. Abe, Y., M. Kakizaki, and T. Hideshima. "Mechanical Relaxation of Polyvinylidene Fluoride and Copolymer of Vinylidene Fluoride and Tetrafluoroethylene in α and β Relaxation Regions." Japanese Journal of Applied Physics 24.2 (1985) 208-213.
27. Goldberg, R.L. and S.W. Smith. The Biomedical Engineering Handbook. New York: IEEE Press, 2000.
28. Suttle, N. "New Piezoelectric Polymers." Materials and Design 9.6 (1998) 318-324.
29. Chen, Y., H. Chan, and C.L. Choy. "Nanocrystalline Lead Titanate and Lead Titanate/Vinylidene Fluoride-Trifluoroethylene 0-3 Nanocomposites." Journal of the American Ceramic Society 81.5 (1998) 1231-1236.

30. Callister, W.D. Materials Science and Engineering: An Introduction. 5th ed. New York: John Wiley & Sons, Inc., 2000.

31. Marra, S.P., K.T. Ramesh, and A.S. Douglas. "The Mechanical and Electromechanical Properties of Calcium Modified Lead Titanate / Polyvinylidene Fluoride-Trifluoroethylene 0-3 Composites." Composite Science and Technology 59 (1999) 2163-2173.

32. Zheng, Z., I.L. Guy, and T. Tansley. "Piezoelectric Coefficients of Thin Polymer Films Measured by Interferometry." Journal of Intelligent Material Systems and Structures 9 (1998) 69-73.

33. Fedosov, S.N., and A.E. Sergeeva. "Corona Poling of Ferroelectric and Nonlinear Optical Polymers." Moldavian Journal of the Physical Sciences N2 (2002) 28-31.

34. Markiewicz, E., J. Kulek, and C. Pawlaczk. "Simple Electric Equivalent Circuit Method to Determine Piezoelectric and Elastic Properties of Piezoelectric Polymer Film." IEEE Transactions on Dielectrics and Electrical Insulation 6.3 (1999) 304-308.

35. Zhang, Q.C., H.L. Chan, Q.F. Zhou, and C.L. Choy. "Calcium and Lanthanum Modified Lead Titanate Ceramics and Vinylidene Fluoride-Trifluoroethylene 0-3 Nanocomposites." Journal of the American Ceramic Society 83.9 (2000) 2227-2230.

36. Linares, A., and J.L. Acosta. "Pyro-Piezoelectric Polymer Materials: Effect of the Addition of PVA and/or PMMA on Overall Crystallization Kinetics of PVDF from Isothermal and Non-isothermal Data." European Polymer Journal 31.7 (1995) 615-619.

APPENDIX

A. Characterization

Piezoelectricity is a phenomenon in which the elastic energy contained in a solid body is coupled with the dielectric energy present in the same material. Piezoelectricity is characterized with proportionality coefficients between mechanical and electrical values, or causes and effects. The following sections discuss the theory and physics behind each element of characterization used in this research.

A.1. Axis definition

Because of the anisotropy of piezoelectric materials, coefficients are determined for each direction of the element. Characteristic values are indexed X_{ij}, with i corresponding to the direction of the electrical value measurement, and j corresponding to the direction of mechanical action. The axes of the material are numbered one to three; with one corresponding to the machine direction, two corresponding to the perpendicular planar direction, and three corresponding to the thickness of the element.[22] According to this, a '31' index will characterize an electrical value considered between two sides of the film, and a mechanical stress applied along the length. In most cases, i = 3 because the electrodes are on the planar surface of the sample.

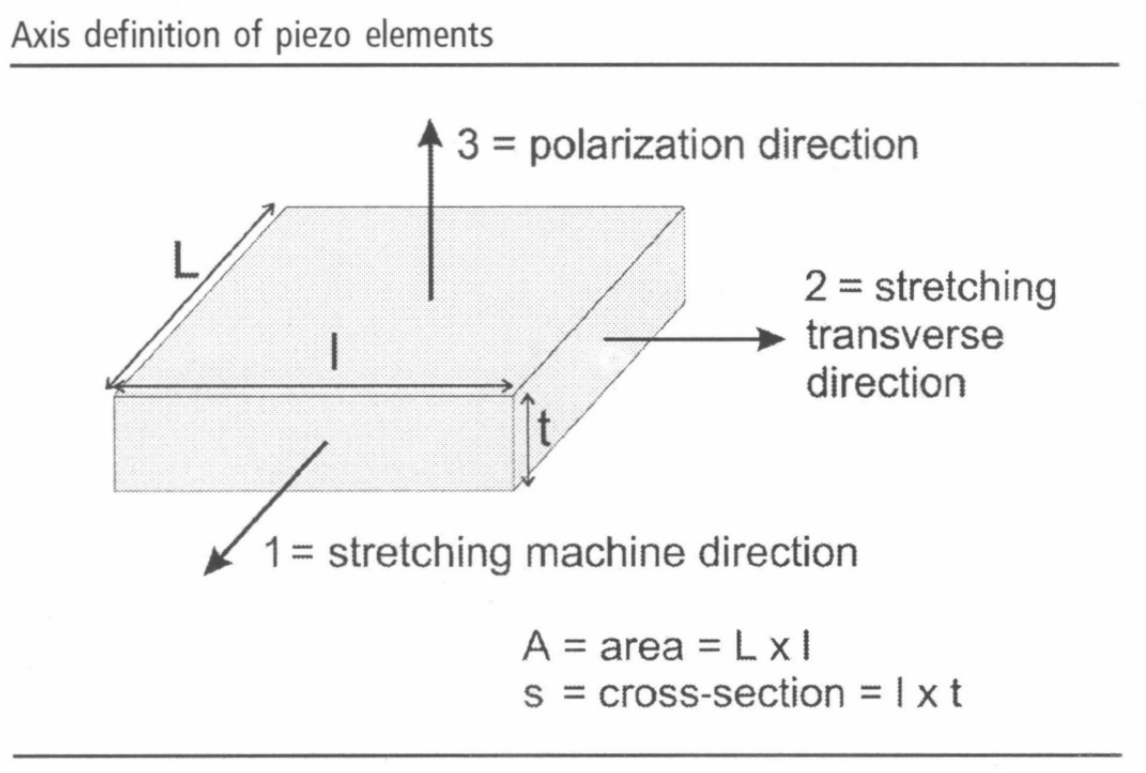

Figure A.1: Axis definition of Piezoelectric Materials

A.2. Impedance

Acoustic impedance is the ratio of sound pressure in a medium to the velocity of the particles in the medium. The acoustic impedance Z of a medium is defined as the product of the density of the medium and the velocity of sound in the medium.

$Z = \rho c$

where Z = acoustic impedance

ρ = density

c = velocity of the sound in the medium

The unit for acoustic impedance is $kg/m^2 \cdot sec$ and is called a Rayl.

When an ultrasonic wave enters a medium, such as tissue, a fraction R of the initial energy is reflected back.

$$R= ((Z_2 - Z_1) / (Z_2 + Z_1))^2 \quad (10)$$

where Z_2 and Z_1 are the acoustic impedance of the transducer material and body, respectively.[18]

Electrical impedance is also an important characteristic of piezoelectric materials. Electrical impedance is defined as the voltage drop across an element, divided by the current that travels through the element. The electrical impedance of piezoelectric materials is greatly different than that of non-piezoelectric dielectric material. This difference results from the combination of electrical energy being added and mechanical motion being produced. The existence of electrical resonances and anti-resonances make the piezoelectric impedance unique. The resonances are a result of the electrical input signal exciting a mechanical resonance. For each mechanical resonance in the piezoelectric material, a resonance and anti-resonance pair will exist in the impedance.[15]

A.3. Piezoelectric Coefficient d

The piezoelectric activity of a sample is indicated by the d_{ij} and measured in Coulomb/Newton. The d_{ij} coefficient corresponds to the electrical charges delivered on the i axis by $1m^2$ when it is exposed to a pressure of 1 Pa along the j axis. Conversely, it also gives the mechanical strain developed along the j axis when an electrical field of 1 V/m is applied along the i-axis. When a sample is clamped along the one and two axis as

referred to above, the dT constant is measured. If the film is used in a hydrostatic atmosphere, the sum of d_{31}, d_{32}, and d_{33} is measured and called dh.[22]

The 'd' coefficient is obtained by measuring the electrical charge density (Coulomb/meter^2), which appears at the surface of the film when a mechanical stress of one Newton/meter^2 is applied. As mentioned above, the resulting value is given in C/N. These constants also correspond to the mechanical strain of the element (meter/meter) compared to the electrical field applied (Volts/meter). The resulting unit here is m/V.

d_{ij}= electrical charge density / applied stress $= \dfrac{Q_i / A_i}{F_j / A_j}$

where

A_x= *area according to x axis*

F= force

Q= charge

d_{ij}= strain / applied electrical field $= \dfrac{\Delta L_j / L_j}{V_i / L_i}$

where

L_x= length according to x axis

V= voltage

Conventionally, mechanical stretching is considered positive and compression is considered negative. A positive electric field corresponds to the direction along which the dipoles are oriented. Accordingly, d_{33} is negative, d_{31} and d_{32} are positive.[22]

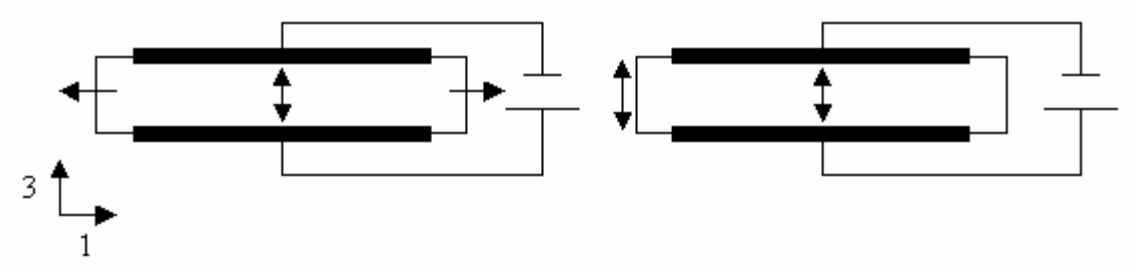

Figure A.2: An illustration of the modes of operation utilizing the **(a)** d_{31} and **(b)** d_{33} dielectric constants.

A.4. Mechanical Coupling Factor k_t

Another important constant for piezoelectric materials is the coupling factor k_{eff}. This is a measure of the effectiveness that mechanical energy is converted into electrical energy, and vice versa. At all frequencies below the resonant frequency of the piezoelectric body, k_{eff} is simply a ratio of the energy converted to the energy input.

k_{eff}^2 = energy converted / energy input

This expression works for both electromechanical and mechano-electrical conversions. Studies of modern piezoelectric ceramics show that up to 50% of the stored energy can be converted at low frequencies, resulting in a k_{eff} of .50.[23]

Although a high k_{eff}^2 is usually desirable for efficient transduction, it is not an absolute measure of the efficiency, because the unconverted energy is not necessarily lost. Usually, unconverted energy results in heat that can be recovered. The real efficiency is the ratio of converted useful energy to the energy absorbed by the transducer. A tuned and well-adjusted transducer working in its resonance region could be more than 90% efficient.

A.5. Leakage

Leakage in a dielectric material is simply a small amount of current traveling through a sample. Dielectric materials are not supposed to conduct electricity, there primary characteristic is the ability to store charge. This capacitive element allows dielectric materials to be used for piezoelectric, capacitive, and insulative applications. If a dielectric material does not have a charge storing capacity, and thus 'leaks', it will have very poor ferroelectric properties. Testing leakage is a primary check to make sure that a material is capable of storing charge, and is connected correctly. Leakage is tested by applying an electrical frequency, over a period of time, to one of the sample electrodes. Any electrical leakage through the sample is recorded from the other electrode. Generally, a ferroelectric ceramic should have about 10^{-8} Amps of leakage in order to produce a good hysteresis loop.

A.6. Hysteresis

The main difference between pyroelectric and ferroelectric materials is that the direction of the spontaneous polarization in ferroelectrics can be switched by an applied electric field. The polarization reversal can be observed by measuring the ferroelectric hysteresis like shown in figure A.3. At low applied fields, the polarization is reversible and almost liner with the applied field. At higher electrical field strengths, the polarization increases due to switching of the ferroelectric domains. As the electric field strength is increased, the domains start to align in the positive direction, causing a rapid increase in the polarization (a_0b). At this point, if a very high electric field is applied, the polarization reaches a saturation value (P_s).[4]

In a ferroelectric material, the polarization does not return to zero when the external field is removed. At zero external field, some of the domains remain aligned in the positive direction, and the crystal will show a remnant polarization P_r. The crystal cannot be completely depolarized until a field of magnitude a_0f is applied in the negative direction. The external field needed to reduce the polarization to zero is called the coercive electric field E_c. If the field is increased to a higher value in the negative direction, the direction of the dipoles flips. A coercive electric field E_c is then needed to return the polarization to zero and produce a complete hysteresis loop. The value of the saturation polarization P_s is obtained by extrapolating the curve onto the polarization axes (bg).[4]

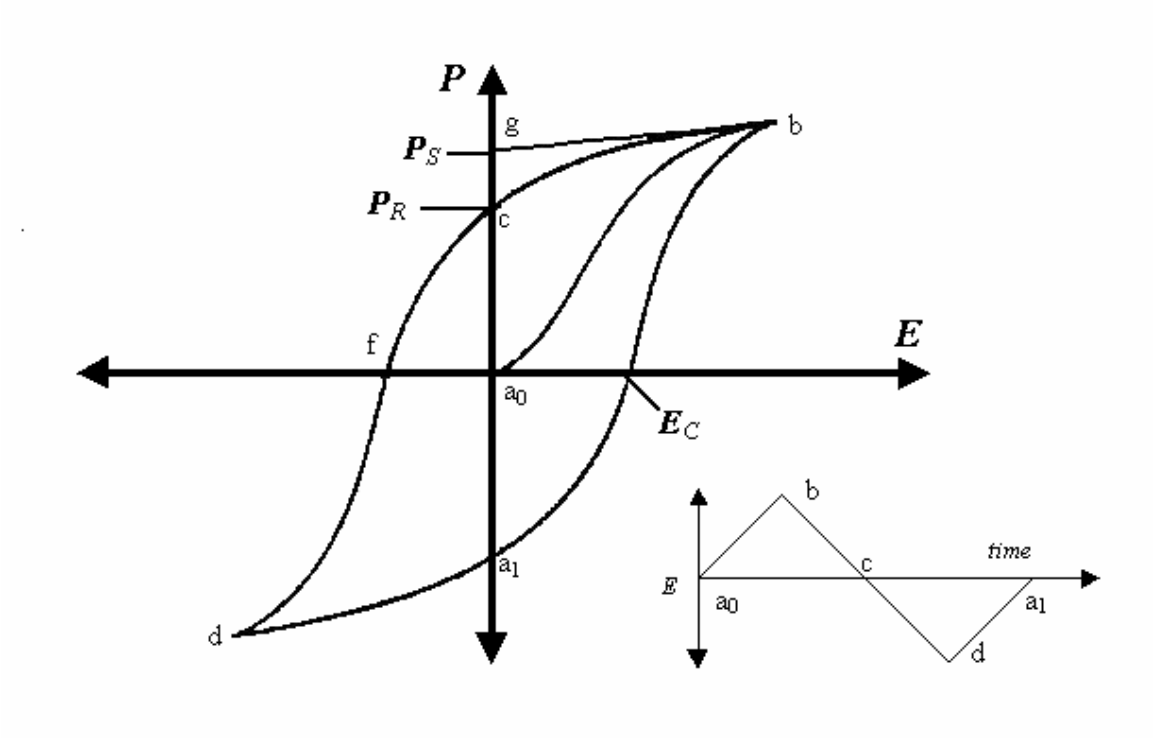

Figure A.3: A Polarization vs. Electric Field (P-E) hysteresis loop for a typical ferroelectric crystal.

One common way of measuring a hysteresis loop is with the use of a testing circuit like the one shown below. A circuit voltage across the ferroelectric crystal is applied to the horizontal plates of an oscilloscope. The vertical plates are attached to a linear capacitor in series with the ferroelectric material. Since the voltage generated across the linear capacitors is proportional to the polarization of the ferroelectric, the oscilloscope will display a hysteresis loop.[3]

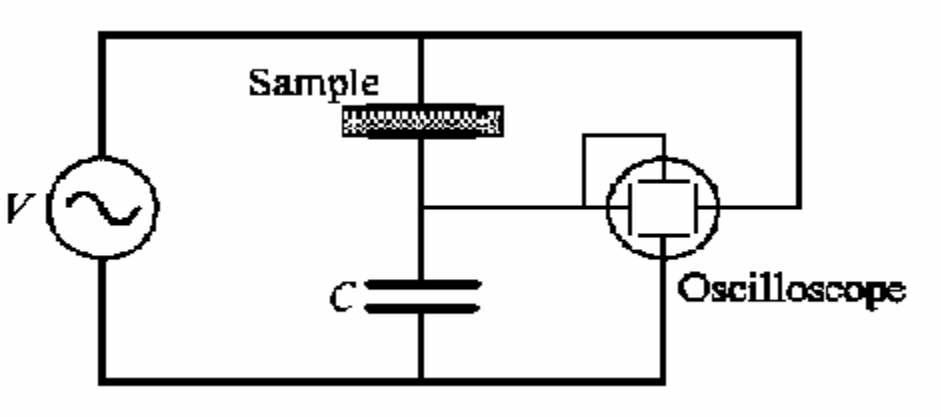

Figure A.4: A diagram showing the circuit used to measure ferroelectric hysteresis.

A.7. Fatigue

Ferroelectric fatigue is the loss of switchable polarization due to repeated switching cycles. The main cause of fatigue in ferroelectric films is domain wall pinning caused by charge carriers in the film. In the presence of an electric field, vacancies become mobile and accumulate at domain walls and grain boundaries. At the domain walls and grain boundaries, the vacancies create localized fields that prevent switching of

neighboring grains.[23] This results in lower remnant polarization values, as shown in the figure below, and a higher dielectric loss.

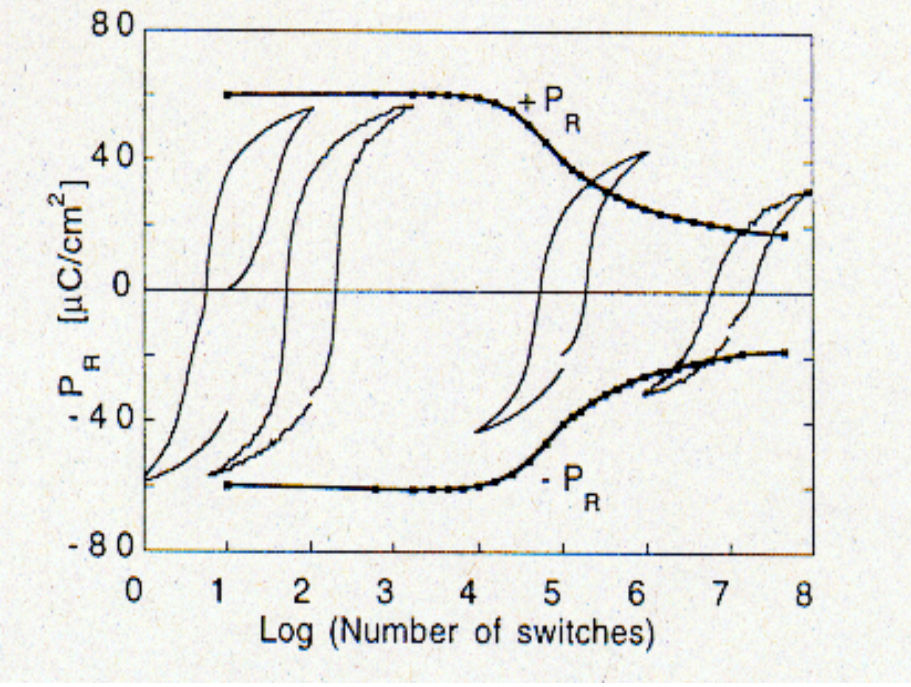

Figure A.5: The degradation of a ferroelectric materials hysteresis behavior as a function of electrical cycles.

B. Properties of Commercial PZT

Dielectric Property	TRS600
K_{33}^{T}	4150
K_{33}^{s}	1495
K_{11}^{T}	4445
K_{11}^{s}	2190
Loss	0.024
T_c (°C)	190
Grain Size (μm)	~ 3 - 5
Q_m	37
d_{33} (pC/N)	675
d_{33} (meter):	
Long Rods	750
Thin Plates	790
d_{31} (pC/N)	-310
d_{15} (pC/N)	850
g_{33} (mm-V/N)	18.3
g_{13} (mm-V/N)	-8.5
g_{15} (mm-V/N)	26
k_{33}	0.76
k_{31}	0.41
k_{15}	0.7
k_p	0.68
k_t	0.58
N_{33} (Hz-m)	1300
N_{31} (Hz-m)	1470
N_p (Hz-m)	1870
N_t (Hz-m)	1925

Elastic Property	TRS600
s_{11}^{E} (m^2/N)	1.55E-11
s_{33}^{E} (m^2/N)	2.12E-11
s_{12}^{E} (m^2/N)	-4.00E-12
s_{13}^{E} (m^2/N)	-8.30E-12
s_{55}^{E} (m^2/N)	4.50E-11
s_{66}^{E} (m^2/N)	3.89E-11
$-s_{12}^{E}/s_{11}^{E}$	0.26
$-s_{13}^{E}/s_{33}^{E}$	0.39
Y_{11}^{E} (GPa)	64
Y_{33}^{E} (GPa)	47
s_{11}^{D} (m^2/N)	1.29E-11
s_{33}^{D} (m^2/N)	8.90E-12
s_{12}^{D} (m^2/N)	-6.60E-12
s_{13}^{D} (m^2/N)	-2.90E-12
s_{55}^{D} (m^2/N)	2.20E-11
s_{66}^{D} (m^2/N)	3.89E-11
c_{11}^{E} (GPa)	126
c_{33}^{E} (GPa)	108
c_{12}^{E} (GPa)	74
c_{13}^{E} (GPa)	78
c_{55}^{E} (GPa)	22
c_{66}^{E} (GPa)	26
c_{11}^{D} (GPa)	142
c_{33}^{D} (GPa)	163
c_{12}^{D} (GPa)	90
c_{13}^{D} (GPa)	77
c_{55}^{D} (GPa)	44
c_{66}^{D} (GPa)	26

Table B.1: Dielectric and elastic properties of commercial TRS 600 PZT commercial powder.[24]

C. Film Spinning Conditions and Results

The table below shows the solution parameters and conditions for mixing and spinning the film samples. The best resultant and standard sized batch for the homopolymer makes about 12 cc of solution. Similarly, the copolymer solution batch size is about 20 cc, and the composite batch makes approximately 10 cc. The homopolymer film is made by adding 4 cc to the center of the silicon wafer on the spin coating machine. As a result, a homopolymer batch makes three film samples. Likewise, the copolymer film takes 4 cc, resulting in five films per batch. The composite material has the thinnest viscosity, so only requires about $3^{1}/_{3}$ cc per sample. A batch of composite solution will make three complete samples. One batch was made for each condition below, resulting in 3 homopolymer films, 5 copolymer films, and 3 composite films for each condition. The average thickness and general comments were made for each batch.

Material	Solvent	Mix Rate and Time	Mix Temperature and Condition	Acceleration / Deceleration	Spin Time and RPM	Appoximate Thickness (μm)	Comments
1.5 g PVDF	10 mL THF	mixed on 3 for 15 min.	uncovered at 23°C	mid-range	60 sec. 500 RPM	29	not completely dissolved solution too thick nonuniform film
1.5 g PVDF	10 mL THF	mixed on 3 for 15 min.	covered at 23°C	mid-range	60 sec. 1500 RPM	18	not completely dissolved solution too thick inconsistent film
1.5 g PVDF	10 mL THF	mixed on 3 for 15 min.	covered at 30°C	mid-range	60 sec. 2500 RPM	13	not completely dissolved good viscosity rough film
1.5 g PVDF	10 mL THF	mixed on 5 for 30 min.	uncovered at 23°C	mid-range	90 sec. 1000 RPM	23	not completely dissolved solution too thick inconsistent film
1.5 g PVDF	10 mL THF	mixed on 5 for 30 min.	covered at 23°C	mid-range	60 sec. 1500 RPM	19	completely dissolved good viscosity smooth film
1.5 g PVDF	10 mL THF	mixed on 5 for 30 min.	covered at 30°C	slower	45 sec. 2000 RPM	15	completely dissolved good viscosity consistent film
1.5 g PVDF	10 mL THF	mixed on 5 for 30 min.	covered at 30°C	faster	45 sec. 2500 RPM	12	completely dissolved good viscosity inconsistent film
1.5 g PVDF	10 mL THF	mixed on 8 for 45 min.	uncovered at 23°C	mid-range	45 sec. 500 RPM	26	not completely dissolved good viscosity nonuniform film

1.5 g PVDF	10 mL THF	mixed on 8 for 45 min.	covered at 23°C	mid-range	45 sec. 1500 RPM	16	completely dissolved good viscosity consistent film
1.5 g PVDF	10 mL THF	mixed on 8 for 45 min.	covered at 30°C	mid-range	45 sec. 2500 RPM	13	completely dissolved good viscosity consistent film
1.5 g PVDF	20 mL THF	mixed on 5 for 30 min.	uncovered at 23°C	slower	90 sec. 1000 RPM	14	completely dissolved solution too thin inconsistent film
1.5 g PVDF	20 mL THF	mixed on 5 for 30 min.	covered at 23°C	faster	60 sec. 1500 RPM	11	completely dissolved solution too thin inconsistent film
1.5 g PVDF	20 mL THF	mixed on 5 for 30 min.	covered at 30°C	mid-range	45 sec. 2000 RPM	9	completely dissolved solution too thin uniform film
1.5 g PVDF	20 mL THF	mixed on 5 for 30 min.	covered at 30°C	mid-range	45 sec. 2500 RPM	5	completely dissolved solution too thin uniform thin film
3.0 g PVDF/TrFE	15 mL THF	mixed on 3 for 15 min.	uncovered at 23°C	mid-range	60 sec. 500 RPM	55	not completely dissolved solution too thick nonuniform film
3.0 g PVDF/TrFE	15 mL THF	mixed on 3 for 15 min.	covered at 23°C	mid-range	60 sec. 1500 RPM	33	not completely dissolved solution too thick inconsistent film
3.0 g PVDF/TrFE	15 mL THF	mixed on 3 for 15 min.	covered at 30°C	mid-range	60 sec. 2500 RPM	27	not completely dissolved good viscosity rough film
3.0 g PVDF/TrFE	15 mL THF	mixed on 5 for 30 min.	uncovered at 23°C	mid-range	90 sec. 1000 RPM	35	not completely dissolved solution too thick inconsistent film
3.0 g PVDF/TrFE	15 mL THF	mixed on 5 for 30 min.	covered at 23°C	mid-range	60 sec. 1500 RPM	27	completely dissolved good viscosity smooth film
3.0 g PVDF/TrFE	15 mL THF	mixed on 5 for 30 min.	covered at 30°C	slower	45 sec. 2000 RPM	25	completely dissolved good viscosity consistent film
3.0 g PVDF/TrFE	15 mL THF	mixed on 5 for 30 min.	covered at 30°C	faster	45 sec. 2500 RPM	22	completely dissolved good viscosity inconsistent film
3.0 g PVDF/TrFE	15 mL THF	mixed on 8 for 45 min.	uncovered at 23°C	mid-range	45 sec. 500 RPM	59	not completely dissolved good viscosity nonuniform film
3.0 g PVDF/TrFE	15 mL THF	mixed on 8 for 45 min.	covered at 23°C	mid-range	45 sec. 1500 RPM	31	completely dissolved good viscosity consistent film
3.0 g PVDF/TrFE	15 mL THF	mixed on 8 for 45 min.	covered at 30°C	mid-range	45 sec. 2500 RPM	25	completely dissolved good viscosity consistent film
3.0 g PVDF/TrFE	25 mL THF	mixed on 5 for 30 min.	uncovered at 23°C	slower	90 sec. 1000 RPM	26	not completely dissolved solution too thin inconsistent film
3.0 g PVDF/TrFE	25 mL THF	mixed on 5 for 30 min.	covered at 23°C	faster	60 sec. 1500 RPM	19	completely dissolved solution too thin consistent film
3.0 g PVDF/TrFE	25 mL THF	mixed on 5 for 30 min.	covered at 30°C	mid-range	45 sec. 2000 RPM	13	completely dissolved solution too thin uniform film

3.0 g PVDF/TrFE	25 mL THF	mixed on 5 for 30 min.	covered at 30°C	mid-range	45 sec. 2500 RPM	9	completely dissolved solution too thin consistent film
1.5 g PVDF/TrFE/PZT	10 mL THF	mixed on 3 for 15 min.	uncovered at 23°C	mid-range	60 sec. 500 RPM	21	not completely dissolved solution too thick nonuniform film
1.5 g PVDF/TrFE/PZT	10 mL THF	mixed on 3 for 15 min.	covered at 23°C	mid-range	60 sec. 1000 RPM	13	not completely dissolved solution too thick inconsistent film
1.5 g PVDF/TrFE/PZT	10 mL THF	mixed on 3 for 15 min.	covered at 30°C	mid-range	60 sec. 1500 RPM	6	completely dissolved good viscosity rough film
1.5 g PVDF/TrFE/PZT	10 mL THF	mixed on 5 for 30 min.	uncovered at 23°C	mid-range	90 sec. 150 RPM	37	not completely dissolved good viscosity inconsistent film
1.5 g PVDF/TrFE/PZT	10 mL THF	mixed on 5 for 30 min.	covered at 23°C	mid-range	60 sec. 300 RPM	26	completely dissolved good viscosity smooth film
1.5 g PVDF/TrFE/PZT	10 mL THF	mixed on 5 for 30 min.	covered at 30°C	slower	45 sec. 600 RPM	20	completely dissolved good viscosity consistent film
1.5 g PVDF/TrFE/PZT	10 mL THF	mixed on 5 for 30 min.	covered at 30°C	faster	45 sec. 900 RPM	14	completely dissolved good viscosity inconsistent film
1.5 g PVDF/TrFE/PZT	10 mL THF	mixed on 8 for 45 min.	uncovered at 23°C	mid-range	45 sec. 600 RPM	19	not completely dissolved good viscosity inconsistant film
1.5 g PVDF/TrFE/PZT	10 mL THF	mixed on 8 for 45 min.	covered at 23°C	mid-range	45 sec. 900 RPM	15	completely dissolved good viscosity consistent film
1.5 g PVDF/TrFE/PZT	10 mL THF	mixed on 8 for 45 min.	covered at 30°C	mid-range	45 sec. 1200 RPM	11	completely dissolved good viscosity consistent film
1.5 g PVDF/TrFE/PZT	20 mL THF	mixed on 5 for 30 min.	uncovered at 23°C	slower	90 sec. 150 RPM	29	not completely dissolved solution too thin inconsistent film
1.5 g PVDF/TrFE/PZT	20 mL THF	mixed on 5 for 30 min.	covered at 23°C	faster	60 sec. 300 RPM	18	completely dissolved solution too thin inconsistent film
1.5 g PVDF/TrFE/PZT	20 mL THF	mixed on 5 for 30 min.	covered at 30°C	mid-range	45 sec. 600 RPM	13	completely dissolved solution too thin uniform film
1.5 g PVDF/TrFE/PZT	20 mL THF	mixed on 5 for 30 min.	covered at 30°C	mid-range	45 sec. 900 RPM	5	completely dissolved solution too thin consistent thin film

Table C.1: Sol-gel preparation and spinning parameters.

D. Poling Information

	Thickness (um)	Poling Field (MV/m)	Leakage at 50 V (Amps)	Electrode Pattern (Sputtered Gold)
PVDF				
1	15	53	10 E-9	one-millimeter dots
2	13	62	10 E-9	one-millimeter dots
3	13	62	10 E-10	two-millimeter lines
4	13	80	10 E-9	two-millimeter lines
5	15	80	10 E-9	two-millimeter lines
6	15	80	10 E-10	two-millimeter lines
7	26	80	10 E-8	two-millimeter lines
8	26	80	10 E-10	two-millimeter lines
9	26	80	10 E-9	two-millimeter lines
PVDF/TrFE				
1	25	32	10 E-9	one-millimeter dots
2	30	27	10 E-10	one-millimeter dots
3	30	27	10 E-10	two-millimeter lines
4	30	80	10 E-10	two-millimeter lines
5	25	80	10 E-9	two-millimeter lines
6	25	80	10 E-9	two-millimeter lines
7	64	80	10 E-10	two-millimeter lines
8	64	80	10 E-10	two-millimeter lines
9	64	80	10 E-9	two-millimeter lines
PVDF/TrFE/PZT				
1	20	40	10 E-10	one-millimeter dots
2	13	62	10 E-9	one-millimeter dots
3	13	62	10 E-10	two-millimeter lines
4	13	80	10 E-9	two-millimeter lines
5	20	80	10 E-8	two-millimeter lines
6	20	80	10 E-10	two-millimeter lines
7	38	80	10 E-9	two-millimeter lines
8	38	80	10 E-10	two-millimeter lines
9	38	80	10 E-9	two-millimeter lines

Table D.1: Sample thickness, poling field, leakage and electrode pattern for each sample summarized in Table 3.1.

E. Peak Polarization

These tables are of the complete information summarized in Table 3.2. The thickness, poling electric field, applied field for testing, and the corresponding peak polarization are shown.

	Thickness	Poling Field	Applied Field (MV/m)	Peak P (uC/cm^2)	Applied Field (MV/m)	Peak P (uC/cm^2)
PVDF	(um)	(MV/m)	at 25 V	of 25 V hysteresis	at 50 V	of 50 V hysteresis
1	15	53	1.667	0.009	3.333	0.022
2	13	62	1.923	0.011	3.846	0.022
3	13	62	1.923	0.008	3.846	0.023
4	13	80	1.923	0.013	3.846	0.026
5	15	80	1.667	0.012	3.333	0.027
6	15	80	1.667	0.010	3.333	0.024
7	26	80	0.962	0.011	1.923	0.022
8	26	80	0.962	0.007	1.923	0.020
9	26	80	0.962	0.009	1.923	0.026
	Thickness	Poling Field	Applied Field (MV/m)	Peak P (uC/cm^2)	Applied Field (MV/m)	Peak P (uC/cm^2)
PVDF/TrFE	(um)	(MV/m)	at 25 V	of 25 V hysteresis	at 50 V	of 50 V hysteresis
1	25	32	1.000	0.018	2.000	0.033
2	30	27	0.833	0.008	1.667	0.022
3	30	27	0.833	0.010	1.667	0.023
4	30	80	0.833	0.012	1.667	0.030
5	25	80	1.000	0.022	2.000	0.039
6	25	80	1.000	0.020	2.000	0.038
7	64	80	0.391	0.012	0.781	0.031
8	64	80	0.391	0.011	0.781	0.029
9	64	80	0.391	0.013	0.781	0.029
	Thickness	Poling Field	Applied Field (MV/m)	Peak P (uC/cm^2)	Applied Field (MV/m)	Peak P (uC/cm^2)
PVDF/TrFE/PZT	(um)	(MV/m)	at 25 V	of 25 V hysteresis	at 50 V	of 50 V hysteresis
1	20	40	1.250	0.034	2.500	0.048
2	13	62	1.923	0.014	3.846	0.029
3	13	62	1.923	0.008	3.846	0.020
4	13	80	1.923	0.018	3.846	0.036
5	20	80	1.250	0.031	2.500	0.054
6	20	80	1.250	0.036	2.500	0.056
7	38	80	0.658	0.030	1.316	0.051
8	38	80	0.658	0.028	1.316	0.044
9	38	80	0.658	0.037	1.316	0.053

	Thickness	Poling Field	Applied Field (MV/m)	Peak P (uC/cm^2)	Applied Field (MV/m)	Peak P (uC/cm^2)
PVDF	**(um)**	**(MV/m)**	**at 75 V**	**of 75 V hysteresis**	**at 100 V**	**of 100 V hysteresis**
1	15	53	5.000	0.031	6.667	0.039
2	13	62	5.769	0.032	7.692	0.042
3	13	62	5.769	0.030	7.692	0.039
4	13	80	5.769	0.033	7.692	0.044
5	15	80	5.000	0.034	6.667	0.041
6	15	80	5.000	0.036	6.667	0.045
7	26	80	2.885	0.024	3.846	0.037
8	26	80	2.885	0.026	3.846	0.039
9	26	80	2.885	0.032	3.846	0.040
	Thickness	**Poling Field**	**Applied Field (MV/m)**	**Peak P (uC/cm^2)**	**Applied Field (MV/m)**	**Peak P (uC/cm^2)**
PVDF/TrFE	**(um)**	**(MV/m)**	**at 75 V**	**of 75 V hysteresis**	**at 100 V**	**of 100 V hysteresis**
1	25	32	3.000	0.041	4.000	0.049
2	30	27	2.500	0.030	3.333	0.039
3	30	27	2.500	0.031	3.333	0.035
4	30	80	2.500	0.036	3.333	0.044
5	25	80	3.000	0.043	4.000	0.053
6	25	80	3.000	0.050	4.000	0.059
7	64	80	1.172	0.039	1.563	0.044
8	64	80	1.172	0.040	1.563	0.049
9	64	80	1.172	0.041	1.563	0.050
	Thickness	**Poling Field**	**Applied Field (MV/m)**	**Peak P (uC/cm^2)**	**Applied Field (MV/m)**	**Peak P (uC/cm^2)**
PVDF/TrFE/PZT	**(um)**	**(MV/m)**	**at 75 V**	**of 75 V hysteresis**	**at 100 V**	**of 100 V hysteresis**
1	20	40	3.750	0.059	5.000	0.071
2	13	62	5.769	0.034	7.692	0.043
3	13	62	5.769	0.027	7.692	0.039
4	13	80	5.769	0.044	7.692	0.053
5	20	80	3.750	0.067	5.000	0.076
6	20	80	3.750	0.063	5.000	0.077
7	38	80	1.974	0.058	2.632	0.069
8	38	80	1.974	0.056	2.632	0.067
9	38	80	1.974	0.060	2.632	0.069

Table E.1: Peak Polarization for nine samples of each type material at four different testing voltages.